Sophie Collard

Design and Assembly of a Thermoacoustic Engine Prototype

Helsinki

Metropolia

University of Applied Sciences

Thermoacoustics combine thermodynamics, fluid dynamics and acoustics to describe the interactions that exist between heat and sound. Under the right conditions, these interactions can be harnessed to design useful devices that convert heat into large amplitude sound waves and vice-versa. A thermoacoustic engine turns part of the heat flowing through a temperature gradient inside a porous solid into sound waves. The work in these sound waves can then be harnessed with a piston to drive a flywheel or a linear alternator, or it can be used to transport heat from a lower to a higher temperature reservoir in what is known as a thermoacoustic heat pump or refrigerator.

Thermoacoustic devices have two major advantages over conventional technologies: their inherent mechanical simplicity, and the use of environmentally friendly working gases. Despite these qualities, most thermoacoustic engines, heat pumps and refrigerators built to this day were for research purposes, and are seldom encountered in the industry.

This thesis documents the design and assembly of a low cost traveling wave thermoacoustic engine prototype intended for low temperature waste heat recovery. Basics of oscillatory motion, acoustics and thermoacoustics are reviewed in chapter 2. Chapter 3 documents the design and assembly of the prototype while chapter 4 details how the engine's performance and efficiency will be calculated using experimental data. Finally, chapter 5 provides conclusions and recommendations for future work.

Metropolia
Helsinki
University of Applied Sciences

Acknowledgement

First and foremost, I wish to thank Fortum Foundation for awarding me a very generous scholarship without which this thesis project could not have been carried out.

I am very thankful to my two supervisors, Antti Tohka and Dr. Minna Paananen-Porkka, for helping me put this thesis together. Thanks to Dr. Kari Vierinen and Hannu Turunen for letting me borrow sensors from the physics lab and to Carola Fortelius and Pekka Saranpää for helping me access the microscope in the materials and surface treatment lab. I also wish to thank the head of the Environmental Engineering degree programme Dr. Esa Toukoniitty, the programme coordinator Jenni Merjankari, and every teacher and staff member from the degree programme in Environmental Engineering at Helsinki Metropolia University of Applied Sciences. Your teachings and your assistance throughout the past four years have been invaluable to me!

I want to express my sincere gratitude to Kees de Blok from Aster Thermoacoustics, who helped me numerous times in dimensioning the engine prototype and in choosing the regenerators material. I cannot go without thanking my former colleagues at FACT Foundation: Winfried Rijssenbeek, Ywe J. Franken, Querine Coenen, Liliana Ruiz, Sandra Bos, Bart Frederiks and J.B. Buquet. Thank you for introducing me to thermoacoustics and for the five amazing months I spend working with you in Eindhoven!

I cannot thank Maija Luostarinen enough for helping me take my first steps in Finland five years ago and for her unconditional support since then. Last but not least, I wish to thank my parents, Monique and Jean-Paul Collard, for being the coolest and most supportive parents I know of!

Sophie Collard
Vantaa, Finland

Nomenclature

Latin capital letters

D_{wire}	mesh wire diameter	mm
F_A	driving force amplitude	N
$F_{driving}$	driving force	N
$F_{restoring}$	restoring force	N
L	length	m
P_{ac}	instantaneous acoustic power	W
$\bar{P}_{ac}$	mean acoustic power	W
$\bar{P}_{el}$	mean electrical power	W
R	resistance	Ω
R_h	hydraulic radius	mm
T	time period of oscillation	s
T_C	temperature on the cool side of the regenerator	K
T_H	temperature on the hot side of the regenerator	K
U	particles volumetric flow rate	$m^3 \cdot s^{-1}$
U_A	particles volumetric flow rate amplitude	$m^3 \cdot s^{-1}$
V	voltage	V
Z	acoustic impedance	$Pa \cdot s \cdot m^{-3}$
Z_0	characteristic acoustic impedance	$N \cdot s \cdot m^{-3}$

Latin lower case letters

a	acceleration	$m \cdot s^{-2}$
b	viscous damping coefficient	$N \cdot s \cdot m^{-1}$
c	speed of propagation	$m \cdot s^{-1}$
c_p	specific heat capacity at constant pressure	$J \cdot kg^{-1} \cdot K^{-1}$
e	percentage of the Carnot efficiency	%
f	frequency	Hz or s^{-1}
k	thermal conductivity	$W \cdot m^{-1} \cdot K^{-1}$
k_s	spring constant	$N \cdot m^{-1}$
k_w	wave number	$rad \cdot m^{-1}$
m	mass	kg
n	mesh number	mm^{-1}
p	acoustic pressure	Pa
p_A	acoustic pressure oscillation amplitude	Pa

p_m	absolute mean pressure	Pa
t	time	s
u	particles velocity	$m \cdot s^{-1}$
u_A	particles velocity peak amplitude	$m \cdot s^{-1}$
x	position or displacement from equilibrium	m
x_A	displacement amplitude	m
z	specific acoustic impedance	$N \cdot s \cdot m^{-3}$

Greek capital letters

$\emptyset$	porosity	%

Greek lower case letters

γ	viscous damping coefficient to mass ratio	s^{-1}
δ_κ	thermal penetration depth	m
δ_ν	viscous penetration depth	m
ζ	damping ratio	dimensionless
η	overall efficiency	%
η_{Carnot}	Carnot efficiency	%
λ	wavelength	m
μ	dynamic viscosity	$N \cdot s \cdot m^{-2}$
ρ_m	mean density	$kg \cdot m^{-3}$
σ	Prandtl number	dimensionless
ϕ	phase angle	rad or °
ϕ_p	phase angle of acoustic pressure oscillations	rad or °
ϕ_u	phase angle of particles velocity oscillations	rad or °
ω	angular frequency	$rad \cdot s^{-1}$
ω_0	natural angular frequency	$rad \cdot s^{-1}$
ω_F	angular frequency of driving force	$rad \cdot s^{-1}$
ω_u	underdamped angular frequency	$rad \cdot s^{-1}$

Abbreviations

ADC	Analogue-Digital Converter
COP	Coefficient Of Performance
IDE	Integrated Development Environment
RMS	Root Mean Square

Contents

Appendices

1   Introduction

Thermoacoustics combine thermodynamics, fluid dynamics and acoustics to describe the interactions that exist between heat and sound. Under the right conditions, these interactions can be harnessed to design useful devices that convert heat into large amplitude sound waves and vice-versa. A thermoacoustic engine turns part of the heat flowing through a temperature gradient inside a porous solid into sound waves. The work in these sound waves can then be harnessed with a piston to drive a flywheel or a linear alternator, or it can be used to transport heat from a lower to a higher temperature reservoir in what is known as a thermoacoustic heat pump or refrigerator.

Thermoacoustic devices have two major advantages over conventional technologies: their inherent mechanical simplicity, and the use of environmentally friendly working gases. Despite these qualities, most thermoacoustic engines, heat pumps and refrigerators built to this day were for research purposes, and are seldom encountered in the industry. This thesis documents the design and assembly of a low cost traveling wave thermoacoustic engine prototype intended for low temperature waste heat recovery. The prototype will later be tested at four different internal mean pressures (ranging from atmospheric to 3 bars gauge pressure) and with one, two, three and four regenerator units in order to measure how these parameters affect the performance of a low cost engine. The test results will be published in a separate document.

Increasing a thermoacoustic engine's internal mean pressure is a well-known way to improve its performance. However, the rate at which acoustic power in the engine increases with increasing internal mean pressure tends to decrease with increasing internal mean pressure and to eventually reach a maximum. Increasing an engine's internal mean pressure also means that the engine's capital cost will be higher, as stronger materials have to be used to ensure a good seal. In the European Union, the manufacturing of pressurized devices is regulated by the Pressure Equipment Directive 97/23/EC, which requires that the equipment be subject to conformity assessment procedures that may in turn drive the capital costs up.

The toroidal geometry of traveling wave thermoacoustic engines makes it possible, in principle, to insert an arbitrary number of regenerators inside the engine's feedback loop, in an effort to increase acoustic gain and improve performances at lower tem-

peratures. The regenerators in today's most efficient thermoacoustic devices are usually built from metal mesh screens stacked together. Metal mesh is a very costly material, and the process of cutting and assembling the screens together is a labor intensive one. In the absence of mass manufacturing techniques that would allow reducing both materials and labor costs of manufacturing regenerators, they will clearly be the most expensive component in a low cost engine. The number of regenerators used is thus of primary importance when optimizing the design of a low cost thermoacoustic device to reach the best possible capital cost per power output ratio.

This thesis was written assuming that the reader has no previous knowledge of acoustics. Thus chapter 2 provides a quick review of oscillatory motion, acoustics and thermoacoustics. Chapter 3 documents the design and assembly of the prototype, including the selection of sensors that will be used to perform the tests. Chapter 4 details how the engine's performance and efficiency will be calculated using the experimental data. Finally, chapter 5 provides conclusions and recommendations for future work.

2   Background

Morin (2011, p. 1) defines a wave as a "correlated collection of oscillations". In sound waves, fluid particles oscillate back and forth about an equilibrium position, giving rise to pressure, density and temperature oscillations. This chapter provides the theoretical background required for understanding the work reported in the following chapters. It is assumed that the reader has no previous knowledge of acoustics. Thus, this chapter starts by reviewing simple harmonic motion, which is at the root of any oscillatory motion, before moving onto damped and driven harmonic motions, acoustics, and finally thermoacoustics. The last section of this chapter, which covers thermoacoustics, is only a very brief introduction to the topic. It provides a qualitative description of the working mechanisms in both standing wave and traveling wave thermoacoustic engines and heat pumps. The complicated quantitative descriptions are voluntarily omitted, as they are beyond the scope of this thesis. Readers interested in a complete overview thermoacoustics are referred to the book *Thermoacoustics: A unifying perspective for some engines and refrigerators* by Greg Swift. The book can be purchased from the Acoustical Society of America, either as a paperback or as a pdf file.

2.1   Oscillatory motion

When a system is displaced from its equilibrium state, forces and torques tend to restore that equilibrium. However, the system being "pulled back" towards equilibrium often overshoots this equilibrium and goes into oscillatory motion. Such system is said to be underdamped. In the absence of friction, these oscillations would continue forever. In real-life, however, the oscillations' amplitude tends to decrease with time and the system eventually settles back into equilibrium. This phenomenon is known as damping.

Oscillatory motion is a periodic motion, that is, motion that repeats itself over and over and is characterized by the time period T that it takes for it to repeat itself in the exact same way. The inverse of the time period T, expressed in seconds, is the frequency of oscillation f, measured in Hertz:

$$f = 1/T \tag{2.1}$$

The frequency is an indication of the number of oscillation cycles that occur within one second.

2.1.1 Simple harmonic motion

Simple harmonic motion is a type of oscillatory motion in which the only forces acting on a system displaced from its equilibrium state are restoring forces directly proportional to the negative value of the displacement. Simple harmonic motion is sinusoidal in time. Both the cosine and sine functions are sinusoids, with the cosine leading the sine by π / 2 or 90°, and are used to quantify simple harmonic motion. Since the exponential function can be expressed as the sum of a cosine and a sine, so that $e^{i\vartheta} = \cos\vartheta + i\sin\vartheta$ (Euler's formula) where $i = \sqrt{-1}$ is the imaginary unit, simple harmonic motion can also be mathematically described using exponentials. In addition to restoring forces, harmonic oscillators may also experience damping and/or driving forces. Remarkably, damped and/or driven harmonic motion provides a good description of most oscillating systems encountered in the real world, provided that the displacement from equilibrium is small (Wolfson 2012, p. 206). Also remarkable is that simple harmonic motion is at the root of any oscillatory motion. This stems from the fact that, as demonstrated by French mathematician Joseph Fourier, any periodic function with frequency f can be expressed as a sum of sinusoidal functions with frequencies f, $2f$, $3f$, ... , nf (Crowell 2002, p. 53). Thus, any oscillatory motion can be described by the superposition of simple harmonic motions.

Consider a mass attached to a spring oscillating back and forth horizontally about an equilibrium position. For now, damping forces are neglected. Hooke's law tells us that $F_{restoring}(x) = -k_s x$ where $F_{restoring}(x)$ is the position-dependent restoring force exerted by the spring on the mass, k_s is a constant and x is the position variable (the distance from equilibrium position $x = 0$). According to Newton's second law, we also have $\sum F = ma$ where $\sum F$ is the sum of all forces acting on the system, m is the mass of the oscillating mass, and a is its acceleration, which is defined as the second derivative of the position x so that $a = d^2x/dt^2$. Thus, it is possible to write that

$$m\frac{d^2x}{dt^2} = -k_s x \qquad (2.2)$$

Solving for x requires finding a function whose second derivative is proportional to the negative of itself. Cosines and sines have this property. Using a cosine function, a solution to Equation 2.2 can be written in the following form:

$$x(t) = x_A \cos(\omega t + \phi) \tag{2.3}$$

where

$$\omega = \sqrt{k_s/m} = 2\pi f \tag{2.4}$$

ω is the angular frequency of oscillation, expressed in radians or degrees per second. x_A and ϕ are the amplitude and phase, respectively, and are arbitrary constants determined by the two initial conditions (position and velocity). The amplitude is defined as the maximum displacement from equilibrium. In the system described by Equation 2.3, the value of the position variable x oscillates between $-x_A$ and x_A. The phase, expressed in radians or in degrees, is a measure of the position at $t = 0$. For a cosine function, if at $t = 0$ the position is $x(0) = x_A$, then $\phi = 0 \text{ rad} = 0°$. If at $t = 0$, $x(0) = -x_A$, then $\phi = \pi \text{ rad} = 180°$. If at $t = 0$, $x(0) = 0$, then ϕ is equal to either $\pi/2 \text{ rad} = 90°$ or $-\pi/2 \text{ rad} = 270°$, depending on whether the mass is traveling from positive to negative x values, or from negative to positive x values.

2.1.2 Damped harmonic motion

Consider the same mass-spring system as in section 2.1.1, only this time in addition to the restoring force exerted by the spring, the mass is also subjected to a damping force proportional to its velocity. Equation 2.2 becomes

$$m\frac{d^2x}{dt^2} = -k_s x - b\frac{dx}{dt} \tag{2.5}$$

where b is a constant known as the viscous damping coefficient and expressed in $N \cdot s \cdot m^{-1}$. Note that a damping force proportional to the mass' velocity is a good representation of the damping force experienced by a solid moving through a fluid at moderate velocity, but is not a representation of the friction force this solid may experience while moving on top of another solid surface, as such friction force would be independent of velocity.

Moving all the terms on the left hand side and dividing by m, Equation 2.5 becomes

$$\frac{d^2x}{dt^2} + 2\zeta\omega_0\frac{dx}{dt} + \omega_0^2 x = 0 \tag{2.6}$$

where

$$\omega_0 = \sqrt{k_s/m} = 2\pi f \tag{2.7}$$

is the natural angular frequency of oscillation and

$$\zeta = \frac{b}{2\sqrt{k_s m}} \tag{2.8}$$

is the damping ratio. Depending on ζ value, the oscillating system exhibits different behaviors. For $\zeta > 1$, the system is said to be overdamped and returns to equilibrium slowly and without going into oscillatory motion. The larger ζ, the longer it takes for the system to return to equilibrium. For $\zeta = 1$, the system is said to be critically damped and returns to equilibrium as quickly as possible but without going into oscillatory motion. For $0 < \zeta < 1$, the system is said to be underdamped and goes into oscillatory motion of decreasing amplitude before eventually settling back into equilibrium. For $\zeta = 0$, the system is said to be undamped and goes into simple harmonic motion, maintaining a constant oscillation amplitude over time.

For an underdamped oscillating system, a solution to Equation 2.6 is of the form

$$x(t) = x_A e^{-\gamma t/2}\cos\left(\omega_u t + \phi\right) \tag{2.9}$$

where

$$\gamma = b/m \tag{2.10}$$

and

$$\omega_u = \frac{1}{2}\sqrt{4\omega_0^2 - \gamma^2} \tag{2.11}$$

ω_u is known as the underdamped angular frequency of oscillation. The factor $\mathrm{e}^{-\gamma t/2}$ shows that the amplitude decreases exponentially with time.

2.1.3 Damped and driven harmonic motion and resonance

Consider the same damped mass-spring system as in section 2.1.2, only this time a driving force $F_{driving}(t) = F_A \cos{(\omega_F t + \phi_F)}$ is added. Equation 2.5 becomes

$$m\frac{d^2x}{dt^2} = -k_s x - b\frac{dx}{dt} + F_A \cos{(\omega_F t + \phi_F)} \qquad (2.12)$$

where F_A is the amplitude of the driving force, ω_F is its angular frequency, and ϕ_F is its phase angle.

A special case when $\omega_F = \omega_0$ and the driving force is in phase with the mass velocity is known as resonance. Since the displacement x is always 90° behind the velocity dx / dt, we have $\phi_F = \phi + \pi/2$. Choosing $\phi_F = 0$, the solution to Equation 2.12 takes the form

$$x(t) = x_A \cos{(\omega_F t + \phi)} \qquad (2.13)$$

$$x(t) = \frac{F_A}{\gamma m \omega_0} \cos{(\omega_F t - \pi/2)} \qquad (2.14)$$

$$x(t) = \frac{F_A}{\gamma m \omega_0} \sin{(\omega_F t)} \qquad (2.15)$$

At resonance, the driving force and mass velocity are in phase. This implies that the force is always performing positive work on the mass, pointing to the right whenever the mass is moving to the right and pointing to the left whenever the mass is moving to the left. For any other phase, there are times when the force is doing negative work, that is, times when the mass is performing work on the force. Because the driving force performs the largest possible amount of work on the system at resonance, the amplitude is the greatest possible and takes the value $F_A/\gamma m \omega_0$. Therefore, thermoacoustic engines are typically dimensioned to produce a wave at a frequency as close as possible to their linear alternators' natural frequency, in order to harness the largest possible amount of energy from the acoustic wave.

2.2 Acoustics

Sound waves are mechanical longitudinal waves, that is, waves which require a medium to propagate and in which the direction of propagation is parallel to the direction of deformation. In addition to particles position oscillations, a sound wave propagating in a fluid involves pressure, density and temperature oscillations. In ideal gases, the speed at which sound propagates is given by

$$c = \sqrt{\gamma_{gas} \cdot \frac{p_m}{\rho_m}} \tag{2.16}$$

where p_m is the mean pressure in the gas, ρ_m the mean density, and γ_{gas} is the gas' ratio of specific heats which has a value of 5/3 for monatomic gases and 7/5 for diatomic gases such as nitrogen and oxygen that make up about 99 % of the air around us.

ρ_m is given by

$$\rho_m = \frac{p_m}{R_{gas} \cdot T_{gas}} \tag{2.17}$$

where R_{gas} is the specific gas constant, which is 287.058 J·kg⁻¹·K⁻¹ for dry air, and T_{gas} is the temperature of the gas, expressed in Kelvins.

2.2.1 The wave equation

The behavior of a wave propagating in a medium in three dimensions is described in the following partial differential equation, known as the wave equation:

$$\nabla^2 \psi - \frac{1}{c^2} \frac{\partial^2 \psi}{\partial t^2} = 0 \tag{2.18}$$

where ∇^2 is the Laplace operator which in three-dimensional x, y, z Cartesian coordinates is defined as $\nabla^2 \psi = \frac{\partial^2 \psi}{\partial x^2} + \frac{\partial^2 \psi}{\partial y^2} + \frac{\partial^2 \psi}{\partial z^2}$, $\psi = \psi(x, y, z, t)$ is the oscillating physical quantity which in the case of a sound wave is typically either the acoustic pressure p

(defined as the local deviation from ambient pressure) or the particles velocity u, c is the speed at which the wave propagates, and t is the time variable.

One dimension is often enough to describe the behavior of a sound wave propagating inside a duct whose lateral dimensions are much smaller than the wavelength, so that the wave is nearly uniform in the transverse y and z directions. Such waves are known as plane waves. For a plane wave, Equation 2.18 simplifies to

$$\frac{\partial^2 \psi}{\partial x^2} - \frac{1}{c^2}\frac{\partial^2 \psi}{\partial t^2} = 0 \qquad (2.19)$$

Provided that c is constant, any solution to Equation 2.19 is of the form

$$\psi(x,t) = f(x - ct) + g(x + ct) \qquad (2.20)$$

where f and g are any two twice-differentiable functions that describe the behavior of two waves traveling in opposite direction, f in the positive x direction and g in the negative x direction.

The wavelength λ is the distance in space over which the motion repeats itself, and is defined as the speed of propagation divided by the frequency

$$\lambda = c/f \qquad (2.21)$$

Another useful quantity when describing the behavior of sound waves is the wave number k_w (not to be confused with the spring constant k_s), defined as

$$k_w = 2\pi/\lambda \qquad (2.22)$$

Using the wave number k_w and the angular frequency of oscillation $\omega = \sqrt{k/m} = 2\pi f$, Equation 2.20 can be written as

$$\psi(x,t) = f\left(x - \frac{\omega}{k_w}t\right) + g\left(x + \frac{\omega}{k_w}t\right) \qquad (2.23)$$

Now, for a sine wave propagating along one dimension, for instance a sound wave propagating inside a duct whose length is much greater than the wavelength, Equation 2.23 becomes

$$\psi(x,t) = \psi_A \cos\left(k_w x - \omega t + \phi\right) + \psi_A \cos\left(k_w x + \omega t + \phi\right) \tag{2.24}$$

where ψ_A is the amplitude and ϕ is the phase angle. Note that Equation 2.24 could also have been written with sine functions instead of cosines, in which case the phase angle would have been φ so that $\varphi = \phi - \pi/2$.

2.2.2 Traveling waves

Consider a sinusoidal sound wave propagating along one dimension inside an infinitely long duct so that the wave never encounters any obstacle and is thus never reflected. The wave propagates along a direction x, going from smaller to greater x values over time. In this case, the term $\psi_A \cos\left(k_w x + \omega t + \phi\right)$ in Equation 2.24 is obviously equal to 0 as there is no wave reflection traveling in opposite direction. Taking this into account and replacing the unknown oscillating physical quantity ψ by the acoustic pressure p, Equation 2.24 becomes

$$p(x,t) = p_A \cos\left(k_w x - \omega t + \phi\right) \tag{2.25}$$

where p_A is the acoustic pressure amplitude. Remember that $p(x,t)$ in the equation above is defined as the acoustic pressure, that is, the local deviation from ambient pressure. If $p(x,t)$ was to represent the absolute pressure at points x in space and t in time while a sound wave propagates inside a medium, the absolute mean pressure of the medium p_m would have to be added to the right-hand-side of the equation.

Particles velocity oscillations are described by the same mathematical expressions as pressure oscillations. The particles velocity oscillations in a sound wave have the same wavelength and frequency as the pressure oscillations, hence the same wave number and angular frequency. In the case of a wave propagating in one dimension inside an infinitely long duct so that it is never reflected, the particles velocity oscillations and the pressure oscillations also have the same phase angle. The particles velocity u at points x in space and t in time is then given by

$$u(x,t) = u_A \cos{(k_w x - \omega t + \phi)} \tag{2.26}$$

where u_A is the particles velocity amplitude. Note that the particles velocity referred to here is the average velocity of a bulk of particles. Naturally, on the microscopic level individual particles inside the bulk move in random directions, but what is interesting here is the average movement of these particles on a macroscopic level.

Waves such as the one described above are called traveling waves since if one looks at either the pressure oscillations or at the particles velocity oscillations over time, the nodes and antinodes in the wave appear to be traveling in positive x direction.

2.2.3 Standing waves

When a sound wave propagates inside a duct with finite length, a reflection will occur when the wave reaches the end of the duct. This will occur no matter whether the end of the duct is closed or open. When both the initial wave and its reflection meet, their pressure and particles velocity oscillation amplitudes are superposed to each other, creating a wave with nearly twice (usually slightly less due to losses) the pressure and particle velocity oscillation amplitudes of the individual traveling waves. This superposition phenomena is called a constructive interference, while the resulting wave is referred to as a standing wave, since if one looks at either the pressure oscillations or at the particles velocity oscillations over time, the nodes and antinodes in the wave appear to be standing still along x direction.

The mathematical representation of acoustic pressure oscillations in a sinusoidal standing wave propagating in one direction is

$$p(x,t) = p_A \cos{(k_w x - \omega t + \phi_p)} + p_A \cos{(k_w x + \omega t + \phi_p)} \tag{2.27}$$

while the mathematical representation of particles velocity oscillations in the same wave is

$$u(x,t) = u_A \cos{(k_w x - \omega t + \phi_u)} + u_A \cos{(k_w x + \omega t + \phi_u)} \tag{2.28}$$

where ϕ_p and ϕ_u are the phase angles of pressure and particles velocity, respectively. In an acoustic standing wave, the particles velocity oscillations lead the pressure oscillations by 90°, so that $\phi_u = \phi_p + \pi/2$.

2.2.4 Acoustic impedance

Although it is usually calculated using the properties of a traveling wave, in non-dispersive media the acoustic impedance is a property of the medium alone, not the wave. In dispersive media, however, the acoustic impedance is determined by both the medium properties and by the frequency of the wave propagating in it. Nitrogen and oxygen that make up about 99 % of the air around us constitute a non-dispersive for audible sound, which is defined as sound waves having frequencies between 20 and 20 000 Hertz.

The acoustic impedance Z is a measure of the force per velocity that a given region of a medium exerts on an adjacent region of this same medium as a wave propagates. Because it is a function of a force, acoustic impedance also is a function of a certain area and thus is a property of a particular geometry of the medium. For a medium inside a duct of cross-sectional area A and in which a one dimensional traveling wave propagates, the acoustic impedance Z is defined as

$$Z = \frac{p}{u \cdot A} = \frac{p}{U} \tag{2.29}$$

where p is the acoustic pressure, u is the particles velocity, and U is the particles volumetric flow rate.

Because acoustic impedance is a property of a medium, it usually makes more sense to express it as a property independent of the particular geometry of the considered medium. In this case, the specific acoustic impedance z defined as the acoustic impedance per area is used:

$$z = Z \cdot A = \frac{p}{u} \tag{2.30}$$

Another useful medium property is the characteristic acoustic impedance Z_0 defined as

$$Z_0 = \frac{p_A}{u_A} = \rho_m \cdot c \tag{2.31}$$

where ρ_m is the density of the medium and c is the speed of sound in this medium.

2.2.5   Acoustic power

The instantaneous acoustic power P_{ac} in a sound wave propagating in one dimension inside a duct having constant cross-sectional area A is given by

$$P_{ac}(x,t) = A \cdot p(x,t) \cdot u(x,t) \tag{2.32}$$

where p is the acoustic pressure and u the particles velocity at points x in space and t in time.

The mean acoustic power $\bar{P}_{ac}$ in the same wave over one or more periods of oscillation is given by

$$\bar{P}_{ac}(x) = \frac{1}{2}A \cdot p_A(x) \cdot u_A(x) \tag{2.33}$$

where $p_A(x)$ and $u_A(x)$ are the position-dependent pressure and particles velocity amplitudes, respectively.

Note that, due to the 90° phase difference between particles velocity and pressure oscillations, a standing wave resulting from the interference between two waves having equal amplitudes carries no net power.

2.3 Thermoacoustics

2.3.1 From Rijke's tube to modern multistage engines

The thermoacoustic effect was probably first observed by glass blowers, who sometimes noticed the generation of a loud sound when connecting a long and narrow blowpipe to a molten glass blob. In 1777, Dr. Bryan Higgins conducted an experiment known as the "singing flame" in which an acoustic standing wave was produced by placing a hydrogen flame inside the lower half of an open glass tube maintained in a vertical position (Beyer 1999, p. 15). In an article published in 1859 in *The London, Edinburgh, and Dublin Philosophical Magazine and Journal of Science*, the Dutch physicist Petrus Leonardus Rijke reports a similar observation, only this time the hydrogen flame was replaced by a hot iron mesh disc. Rijke reports that "In order that the sound may have its maximum intensity, the distance of the disc from the lower end of the tube should be one-fourth of its entire length". He also noted that closing one of the tube's ends would stop the sound, showing that "the presence of an ascending current of air is one of the conditions of the phenomenon" (Rijke 1859, pp. 419-422). Higgin's singing flame and Rijke's tube are depicted in Figure 1.
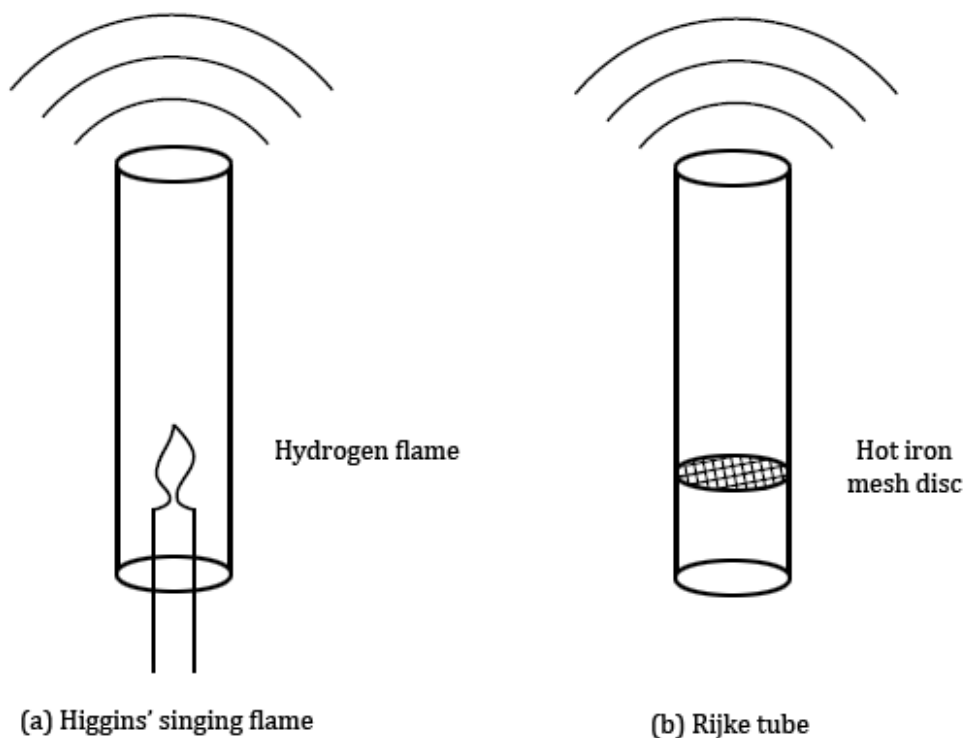

Figure 1. (a) Higgins' singing flame, (b) Rijke's tube (In't panhuis 2009, p. 2)

The earliest known predecessor to today's standing wave thermoacoustic engines was invented by the German physicist Karl Friedrich Julius Sondhauss in 1850. It consists of a long glass tube with one end open and the other end connected to a glass bulb (Figure 2). The tube is maintained in an horizontal position and a gas flame is placed under the bulb. As temperature at the tube's closed end rises, it starts emitting a sound from the open end. Sondhauss' tube differs from Higgins' singing flame and Rijke's tube in that it does not require an ascending air current for the oscillations to occur, and can therefore work in an horizontal position (In't panhuis 2009, p. 3).
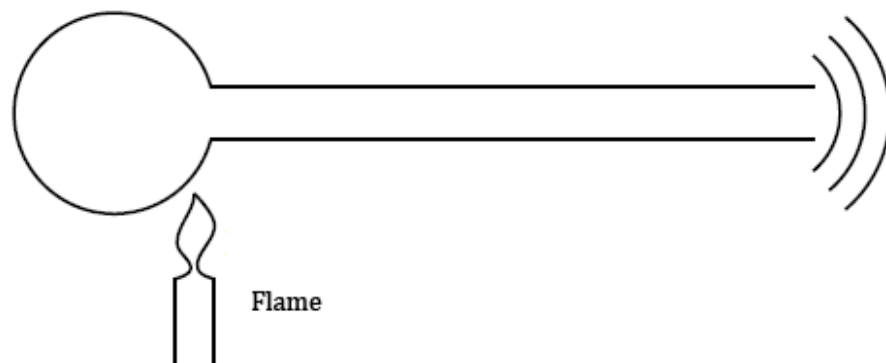

Figure 2. Sondhauss tube (In't panhuis 2009, p. 3)

The performance of the Sondhauss tube was significantly improved in 1962, when Carter et al. tried placing a stack of parallel plates inside the tube, which made it easier to exchange heat with the working gas (In't panhuis 2009, p. 4). In modern thermoacoustic engines, such as the one depicted in Figure 3, heat exchangers are placed on both sides of the stack in order to exchange heat with external reservoirs and maintain a steep temperature gradient across the stack. Part of the heat flowing from the hot to the cool side of the stack is turned into work in the form of an acoustic standing wave. This work can then be extracted with a piston to drive a flywheel or a linear alternator, or it can be used to run a thermoacoustic heat pump or refrigerator.
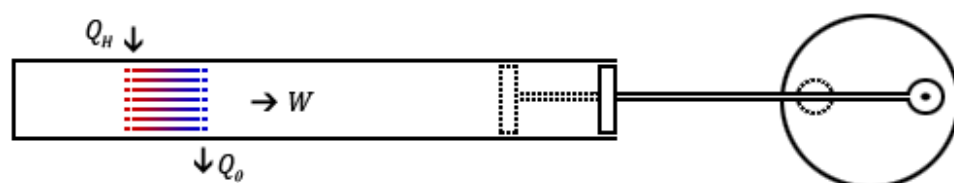

Figure 3. Standing wave thermoacoustic engine

In 1979, Peter H. Ceperley realized that the efficiency of thermoacoustic devices could be further improved by using a toroidal geometry, which would allow for a traveling wave to propagate inside the device instead of a standing wave (In't panhuis 2009, p. 5). One reason for this improvement in efficiency is that a standing wave is the result of a constructive interference between two traveling waves, so that the pressure and velocity amplitudes can be nearly twice the amplitudes in the initial traveling wave generated in the engine, resulting in high acoustic losses (de Blok 2010, p. 2). Ceperley also noted that the gas inside a traveling wave device experiences a similar cycle to the one experienced by the working gas inside a Stirling engine (In't panhuis 2009, p. 5). Thus, traveling wave thermoacoustic engines are sometimes referred to as "acoustic Stirling engines". To exchange heat with the working gas, these devices use a regenerator: a porous material similar to the stack encountered in standing wave devices but with smaller openings. The high and low temperature heat exchangers and the stack or regenerator altogether are sometimes referred to as a "stage". A travelling wave thermoacoustic engine is depicted in Figure 4.
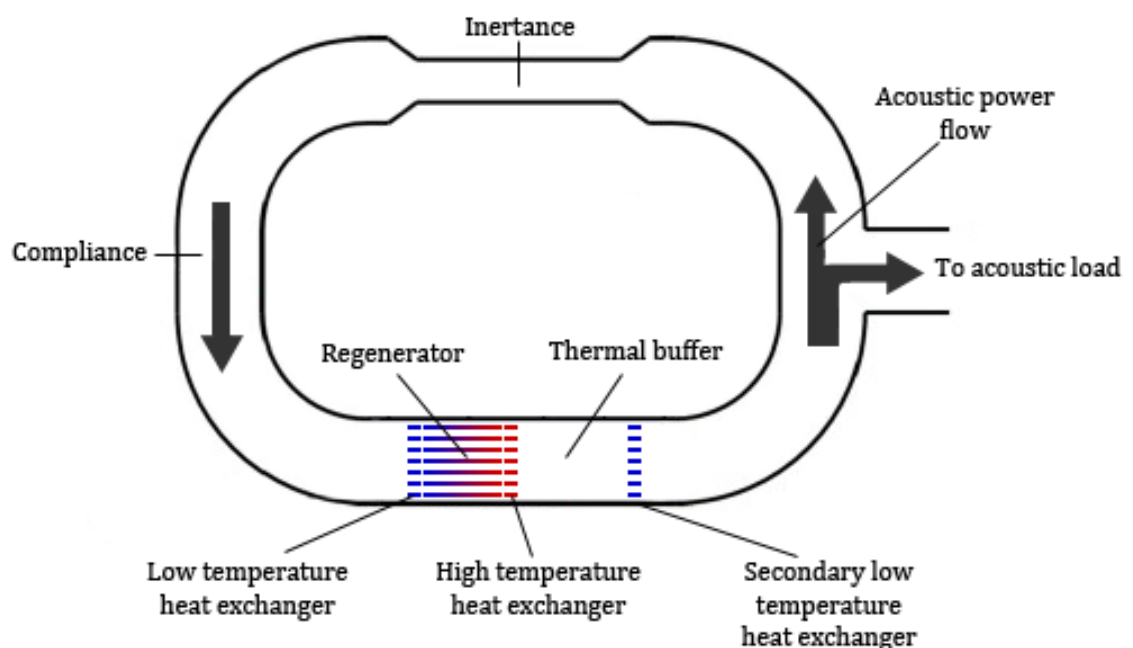

Figure 4. Traveling wave thermoacoustic engine. The inertance and compliance are required to maintain the traveling wave phasing in a single-stage engine. The thermal buffer helps thermally isolating the hot heat exchanger from ambient-temperature components below, thus limiting heat losses.

The toroidal geometry of traveling wave engines makes it possible, in principle, to insert an arbitrary number of regenerators inside the feedback loop, in an effort to increase acoustic gain and improve the engine's performance at lower temperatures.

The drawback of this approach is that in order to maintain optimal acoustic conditions throughout the feedback loop, the dimensions of each regenerator and tube section need to be carefully adjusted, often leading to complex engine geometries (de Blok 2010, pp. 2-3). A special configuration suggested by de Blok, however, is when an even number (typically two or four) of equally spaced regenerators is inserted inside the feedback loop, so that the distance from one regenerator to the other is half of the wave length in the case of a two-stages engine, and a quarter of the wavelength in the case of a four-stages engine (Figure 5). De Blok explains that in this case, "reflections due to impedance anomalies tend to compensate each other" (de Blok 2010, p. 3).
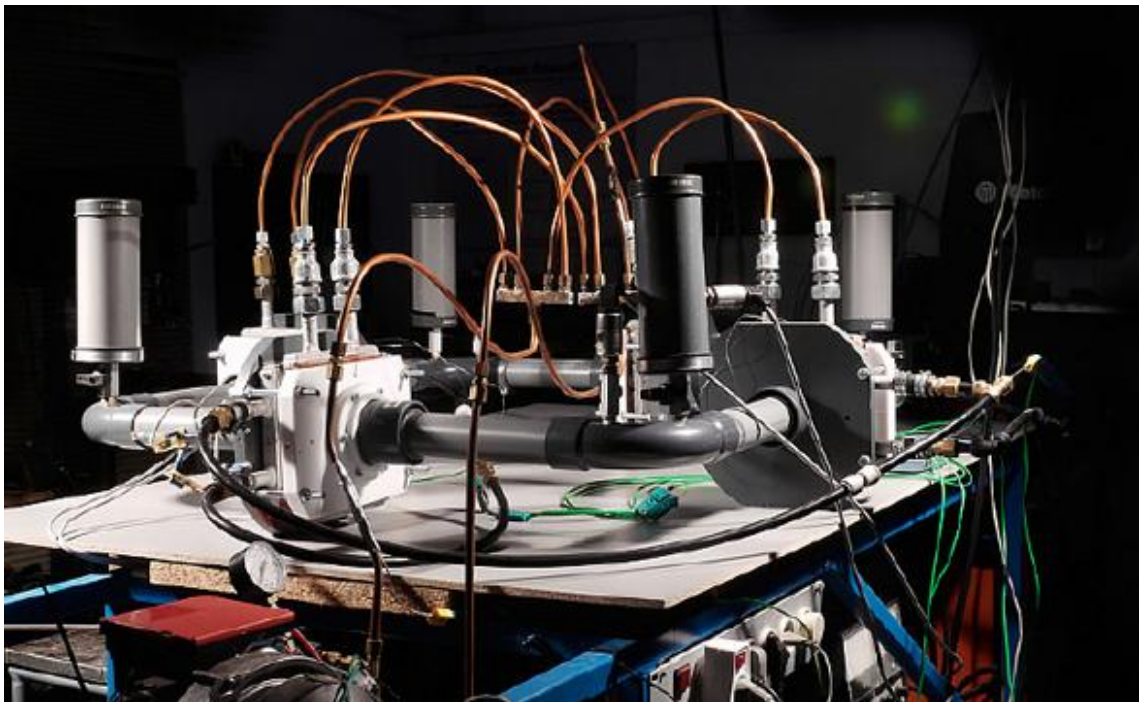

Figure 5. Four-stages traveling wave engine. The engine is filled with air and operates at atmospheric pressure. Acoustic oscillations start when the temperature difference across the regenerator reaches 70°C. (Image courtesy of Aster Thermoacoustics)

If identical and equally-spaced acoustic loads are added to each of the four stages, the engine will be perfectly symmetrical, which is beneficial for mass production. Another interesting feature of this configuration is that, as the phase over one wavelength raises monotonically from 0 to 2π, the phase difference from one load to the other will be π (180°) in a two-stages engine, and $\frac{1}{2}\pi$ (90°) in a four-stages engine. This means that two opposite loads will move in antiphase, cancelling out each other's vibrations.

2.3.2   Important length scales

The wavelength λ of the sound wave's fundamental mode is an important length scale along the wave-propagation direction x. The wavelength depends on the length L of the tube in which the wave propagates and on whether the tube has open or closed ends.

For a tube of finite length and with both ends open, or both ends closed, the wavelength will be twice the length of the tube:

$$\lambda = 2L \tag{2.34}$$

For a tube with finite length and with one end open and the other end closed, the wavelength will be four times the length of the tube:

$$\lambda = 4L \tag{2.35}$$

For a tube with virtually infinite length, i.e. a loop, the wavelength will be equal to the length of the tube:

$$\lambda = L \tag{2.36}$$

Another important length scale along the wave-propagation direction is the displacement amplitude x_A of the gas particles, which is given by dividing the velocity amplitude u_A of the gas particles by the angular frequency of oscillation:

$$x_A = \frac{u_A}{\omega} \tag{2.37}$$

The displacement amplitude is always shorter than the wavelength. Thermoacoustic devices are designed so that the displacement amplitude is often a very large fraction of the stack or regenerator length (Swift 2002, p. 7).

Two important length scales perpendicular to the direction of wave-propagation are the thermal penetration depth and viscous penetration depth. Thermal penetration depth δ_κ is given by

$$\delta_\kappa = \sqrt{\frac{2k}{\omega \rho_m c_p}} \tag{2.38}$$

and viscous penetration depth δ_v by

$$\delta_v = \sqrt{\frac{2\mu}{\omega \rho_m}} \tag{2.39}$$

where k is the gas thermal conductivity, μ is its dynamic viscosity, c_p its specific heat at constant pressure, ρ_m its mean density and ω is the angular frequency of oscillation.

The square of the ratio between the viscous penetration depth and the thermal penetration depth is the Prandtl number and is close to unity for typical gases:

$$\sigma = \left(\frac{\delta_v}{\delta_\kappa}\right)^2 = \frac{\mu c_p}{k} \lessapprox 1 \tag{2.40}$$

Swift (2002, p.7) explains that the thermal and viscous penetration depths indicate how far heat and momentum can diffuse perpendicularly to the wave-propagation direction during a time interval of the order of the period of oscillation T divided by π. In order to exchange heat with the working gas, the channels in stacks have lateral dimensions of the same order as the thermal penetration depth. Regenerators typically have channels whose lateral dimensions are smaller than the thermal penetration depth. Since σ is close to unity for typical gases, the viscous penetration depth δ_v is also of the same order as δ_κ, and thermoacoustic devices usually suffer from substantial viscous losses (Swift 2002, p. 8).

Since the channels' geometry may differ from one stack or regenerator to another, the preferred unit to compare the channels' size to the thermal penetration depth is the channels' hydraulic radius R_h:

$$R_h = D_{wire} \frac{\emptyset}{4(1 - \emptyset)} \tag{2.41}$$

where $\emptyset$ is the material's porosity and is given by

$$\emptyset = 1 - \frac{\pi n D_{wire}}{4} \qquad (2.42)$$

where n is the number of mesh per length unit.

2.3.3 Standing wave heat pumps and refrigerators

Picture a tube of length L with both ends closed such as the one depicted in Figure 6. One end is closed by a loudspeaker which emits a sound with frequency $f = c/2L$, where c is the speed of sound in the gas contained in the tube. Now, it is easy to see that the wavelength λ of the sound wave will be twice the length of the tube. Since the other end of the tube is closed as well, the wave emitted by the loudspeaker will be reflected, and a standing wave will arise. The dotted lines in Figure 6 show the pressure profile in the tube. A stack has been placed at one fourth of the tube's length starting from the left. Below both tube diagrams in Figure 6 is a magnified view of a gas parcel oscillating inside one of the stack's channels.
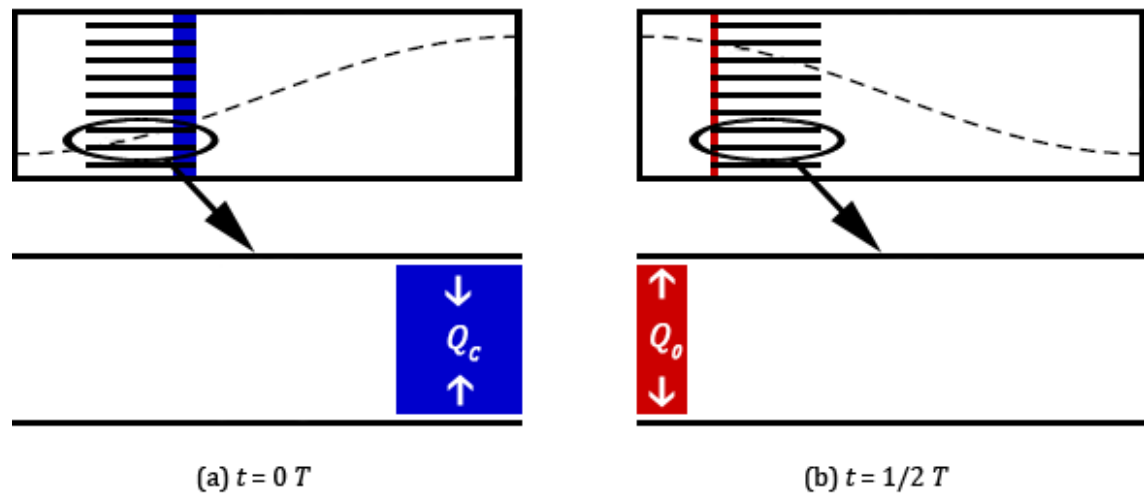

(a) $t = 0\,T$ (b) $t = 1/2\,T$

Figure 6. Standing wave heat pump or refrigerator

At the start of an oscillation, that is at $t = 0\,T$, there is a low pressure in the left half of the tube and the gas parcel inside the stack channel is moved to the right. At this point, the pressure inside the parcel is at its minimum, and so is the temperature. Since the gas parcel is in thermal contact with a solid boundary, whose temperature is higher than that of the parcel, heat will flow from the stack walls into the parcel. This is depicted in Figure 6 (a).

The gas parcel then moves towards the left while shrinking as pressure in the left half of the tube increases. At $t = \frac{1}{2}T$, the pressure inside the parcel is at its maximum, and so is the temperature. The temperature inside the gas parcel being higher than that of the solid boundary, heat will flow from the parcel into the stack walls. This is depicted in Figure 6 (b).

The gas parcel then moves back towards the right, and the process repeats itself as long as the loudspeaker maintains oscillations. By successively removing heat from the right end of the stack and rejecting it at the left end, the sound wave creates a temperature gradient across the stack. If heat exchangers are placed at both ends of the stack in order to exchange heat between the stack and external reservoirs, heat can be pumped from a lower temperature reservoir into a higher temperature reservoir by the thermoacoustic device.

2.3.4   Standing wave engines

Thermoacoustic engines, sometimes referred to as prime movers, use hardware that is identical to that of heat pumps and refrigerators but operate with the reverse process. The heat exchanger that is closest to the tube's end (the one on the left of the stack in Figure 7) is connected to a heat source while the other heat exchanger is connected to a cooling circuit, in order to create a temperature gradient across the stack.
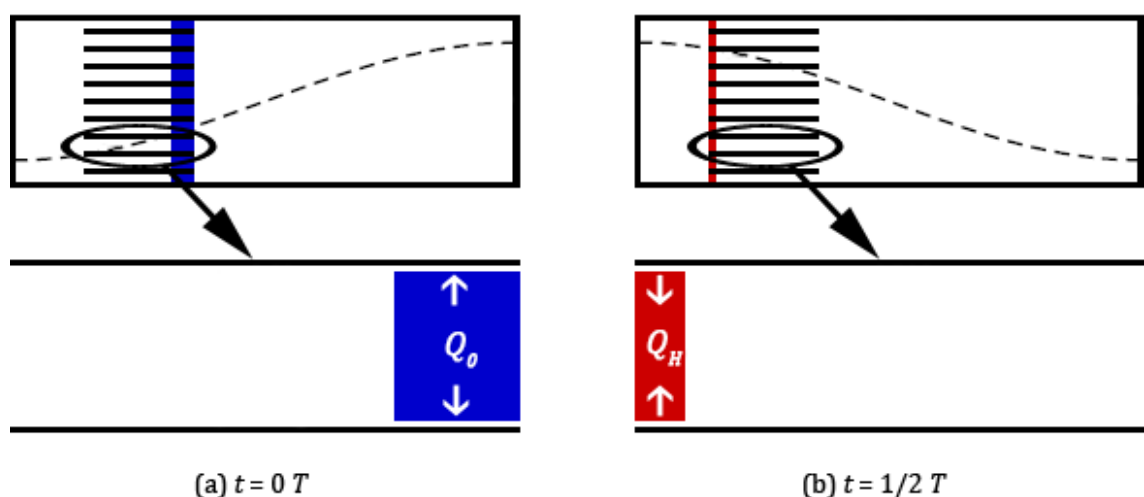

(a) $t = 0\ T$ (b) $t = 1/2\ T$

Figure 7. Standing wave engine

A thermoacoustic engine works as an amplifier. Suppose there were already faint pressure and velocity oscillations in the tube, with wavelength $\lambda = 2L$. At the start of an oscillation, that is at $t = 0\,T$, there is a low pressure in the left half of the tube and the gas parcel inside the stack channel is moved to the right. This time, however, since the oscillations are weak and the gas parcel does not expand so much, the temperature of the parcel is higher than the temperature of the stack walls which are cooled by the heat exchanger connected to the cooling circuit. Thus, heat will flow from the parcel into the stack walls, as depicted in Figure 7 (a).

The gas parcel then moves towards the left while shrinking as pressure in the left half of the tube increases. At $t = \frac{1}{2}\,T$, the pressure inside the parcel is at its maximum, and so is the temperature. However, since the oscillations are weak and the gas parcel does not shrink so much, the temperature of the parcel is lower than the temperature of the stack walls which are heated up by the heat exchanger connected to the heat source. Thus, heat will flow from the stack walls into the parcel, as depicted in Figure 7 (b).

The gas parcel then moves back towards the right, and the process repeats itself as long as the steep temperature gradient across the stack is maintained. When heat is transferred to the parcel at the time when its temperature is the highest and is taken from the parcel at the time when its temperature is the lowest, the amplitude of temperature oscillations in the gas parcel is being increased, and so is the amplitude of pressure oscillations. This phenomenon was described by Lord Rayleigh in his work *The Theory of Sound* which provided the first qualitative explanation for the thermoacoustic effect: "If heat be given to the air at the moment of greatest condensation, or be taken from it at the moment of greatest rarefaction, the vibration is encouraged" (In't panhuis 2009, p. 4).

Swift found that the thermodynamic cycle experienced by the working gas in standing wave devices was similar to the Brayton cycle (In't panhuis 2009, p. 20). A pressure-volume diagram of the idealized Brayton cycle is depicted in Figure 8.
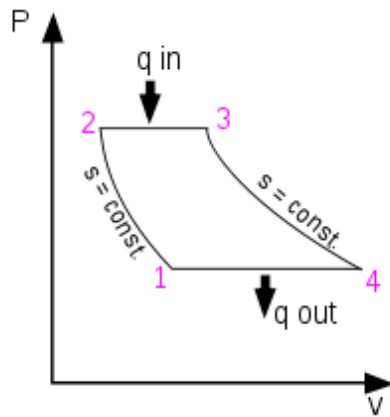
Figure 8. Idealized Brayton cycle (Image courtesy of Wikipedia)

In the idealized Brayton cycle, addition and removal of heat occurs over constant pressure and is accompanied by a volume change. Note that in real-life, the four steps in the cycle are overlapping each other, and the path in Figure 8 resembles an ellipse.

2.3.5   Traveling wave devices

Peter H. Ceperley showed that the gas inside a traveling wave devices experiences a thermodynamic cycle similar to the Stirling cycle. A pressure-volume diagram of the idealized Stirling cycle is depicted in Figure 9.
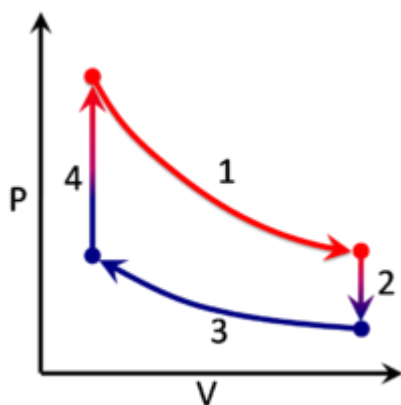

Figure 9. Idealized Stirling cycle (Image courtesy of Wikipedia)

This time, addition and removal of heat occurs over constant volume and is accompanied by a pressure change. Because particles velocity and pressure oscillate in phase in a travelling wave, a very good thermal contact between the gas and the solid sup-

porting a temperature gradient is required to ensure that heat addition and removal stay in phase with the oscillating pressure (Swift 2002, p. 21). This excellent thermal contact is achieved by making the regenerator channels smaller than those of stacks in standing wave engines.

2.3.6 Engines versus heat pumps/refrigerators

Consider a parcel of gas oscillating in a closed tube far away from any solid boundary so that no heat exchange takes place between the parcel and the tube walls. The parcel expands and shrinks in a reversible adiabatic process, which is also an isentropic process. The parcel is also oscillating far from any pressure or velocity node so that it experiences both a displacement around an equilibrium position and pressure oscillations, which under isentropic conditions are accompanied by temperature oscillations. Within thermoacoustics, the slope of these reversible adiabatic temperature oscillations experienced by the parcel is known as the critical temperature gradient, expressed in K·m^{-1}, and is given by

$$\boldsymbol{\nabla} T_{crit} = \frac{\omega A p_A}{\rho_m c_p U_A} \tag{2.43}$$

where $\boldsymbol{\nabla}$ is the gradient operator defined as $\boldsymbol{\nabla} = \frac{\partial}{\partial x}\boldsymbol{i} + \frac{\partial}{\partial y}\boldsymbol{j} + \frac{\partial}{\partial z}\boldsymbol{k}$ in three dimensional x, y, z Cartesian coordinates.

Whether a thermoacoustic device will operate as an engine or as a heat pump or refrigerator depends on the temperature gradient across a section of the stack or regenerator and on the critical temperature gradient of the gas parcel oscillating inside this section. This is depicted in Figure 10.
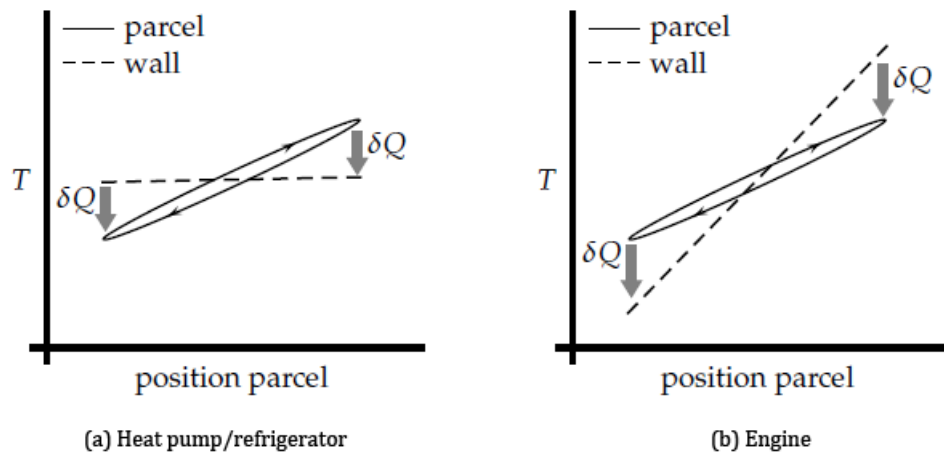
(a) Heat pump/refrigerator (b) Engine

Figure 10.   Heat pump/refrigerator versus engine (In't panhuis 2009, p. 8). Note that in this figure, the hotter side of the stack is located on the right while the cooler side is located on the left.

When the temperature gradient across a section of the stack or regenerator is less steep than the critical temperature gradient of the gas parcel oscillating inside this same section, the parcel will absorb heat at the cold end of the stack section and reject heat at the hot end of the stack section, consuming work in the acoustic wave. In this case, depicted in Figure 10 (a), the thermoacoustic device will operate as a heat pump or refrigerator.

When the temperature gradient across a section of the stack or regenerator is steeper than the critical temperature gradient of the gas parcel oscillating inside this same section, heat will be transferred into the parcel at the hot end of the stack section and removed from the parcel at the cold end of the stack section, transferring work into the acoustic wave. In this case, depicted in Figure 10 (b), the thermoacoustic device will operate as an engine.

Notice that the position-temperature curve of the gas parcel does not follow a straight line but forms an ellipse. This ellipse is proportional to the amount of work performed on the acoustic wave in an engine and to the amount of work performed by the acoustic wave in a heat pump or refrigerator.

2.3.7   Advantages over conventional technologies

Thermoacoustic devices have two major advantages over conventional technologies: their inherent mechanical simplicity, and the use of environmentally friendly working gases. Firstly, while in traditional Stirling engines and in compression heat pumps and refrigerators, massive pistons moved by crankshafts are responsible for harnessing or performing work on the gas, in thermoacoustic devices this is done by an acoustic wave. In the case of devices that involve generating or using electricity, the only moving part required is a linear alternator or a loudspeaker. For devices that run on lower temperature heat and generate higher temperature heat (heat pumps) or cooling (refrigerators), not a single moving part is required. This makes thermoacoustic devices cheaper and more reliable than most traditional technologies. Secondly, unlike traditional vapour-compression or absorbtion systems, thermoacoustic heat pumps and refrigerators do not require using ozone-depleting substances, potent greenhouse gases or toxic and environmentally hazardous chemicals. Instead, they use compressed air or a mixture of noble gases such as helium and argon.

2.3.8   Efficiencies and potential areas of application

Although the efficiencies achieved by modern thermoacoustic devices are not always on par with those of established technologies, it is important to keep in mind that even less efficient technologies may be commercially successful in some markets. Swift (2002, pp. 22-25) cites the example of Stirling refrigerators, which can achieve remarkably high COPs. However, a high COP comes at a great capital cost as high quality components and lubricants are required. The price of energy so far has been low enough, that less efficient but cheaper vapour-compression refrigerators have proven to be commercially more interesting than Stirling refrigerators and are now being used in nearly all commercial refrigeration systems. In the case of applications that use a virtually free fuel, such as solar thermal power or industrial waste heat, the efficiency becomes even less important. The only relevant factor in this case is the cost of generating a certain amount of power, and a less efficient but also cheaper technology may well overtake older and well established ones, provided that it has a lower cost per power output ratio. This is illustrated in Figure 11.
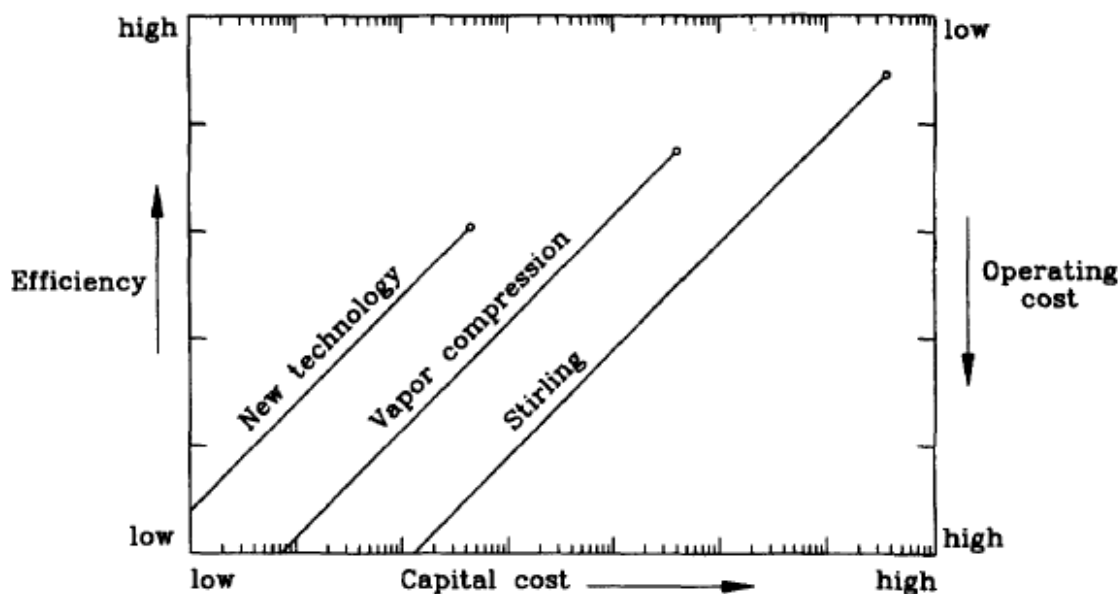
Figure 11.   A new technology may well overtake established ones, provided it has a lower capital cost at useful efficiencies (Swift 2002, p. 25).

Furthermore, choosing a suitable technology for a certain application always involves a trade-off between capital cost and efficiency. For example, it makes sense to invest in an expensive and highly efficient heat pump to heat up a house in Scandinavia, but for a house located in Spain, a cheaper and less efficient heat pump may be sufficient. De Blok (2010, p. 1) identifies utilizing low temperature heat from solar vacuum tube collectors or industrial waste heat in the range 70 to 200 °C as the most promising commercial application for thermoacoustic systems.

3   Design and assembly of the prototype

In order to measure how the internal mean pressure and number of regenerators affect the performance of a low cost thermoacoustic engine, a prototype will be tested at four different pressures (ranging from atmospheric to 3 bars gauge pressure) and with one, two, three and four regenerator units. This chapter details the design and assembly of the engine itself, as well as the selection of appropriate sensors required to perform the tests.

3.1   Thermoacoustic engine

The travelling wave thermoacoustic engine prototype consisted of four pressure vessels, each housing a regenerator clamped between two heat exchangers, a feedback loop connecting the vessels to one another, and a loudspeaker that would serve as a linear alternator. A preview of the engine assembled with four pressure vessels is shown in Figure 12.
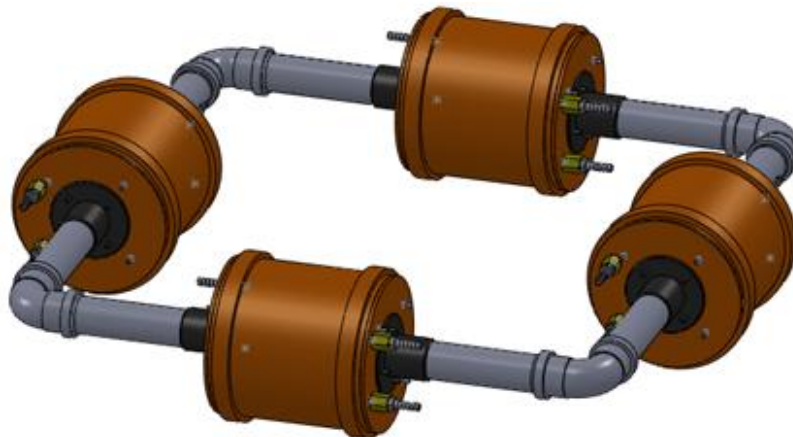

Figure 12.   Thermoacoustic engine prototype assembled with four pressure vessels

An exploded view of one of the pressure vessels, exposing the heat exchangers and the regenerator inside of it, is shown in Figure 13.
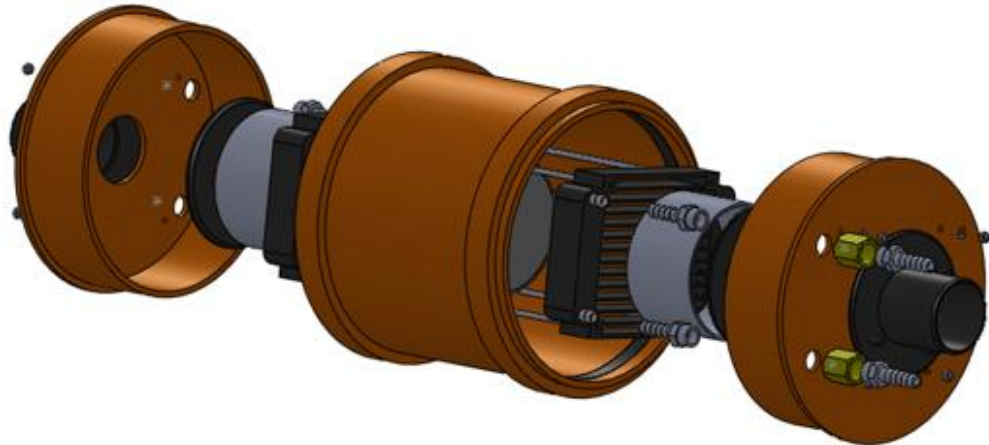
Figure 13.   Exploded view of one of the pressure vessels

The engine had to be easy to assemble and disassemble, so that various configurations could be tested. It also had to withstand internal gauge pressures up to 3 bars. The feedback loop was dimensioned so that the wave generated in the engine would have a frequency of about 120 Hz, which was the resonance frequency of the loudspeaker. The engine was originally designed to run on hot water provided by a solar evacuated tubes collector. However, no such collector was available at the time the tests were performed, and soldering iron heating elements powered by a 230 Volts AC current were used instead to provide heat to the engine. Cooling was provided by tap water.

3.1.1   Pressure vessels and feedback loop

PVC-U drainage pipe sockets with a nominal diameter of 200 mm and matching end plugs were used to build the pressure vessels housing the regenerators and heat exchangers. The sockets and plugs were manufactured by Funke Kunststoffe GmbH and purchased from eBay Germany. The manufacturer's website does not provide any information regarding the maximum temperatures and pressures the pipes can withstand, but the wall thickness was known to be 4.9 mm. Manufacturers Plomyplas (Plomyplas Group, p. 6) and Sirci (Sirci Gresintex, p. 4) both produce PVC-U pipes with similar dimensions having pressure ratings PN6 and Class B, respectively. These ratings both indicate that the pipes are able to withstand gauge pressures of up to 6 bars at 20°C (Morris). At higher temperatures, the strength of PVC decreases and the maximum pressure must be adjusted by a de-rating factor. De-rating factors for temperatures up to 60°C are presented in Table 1.

Table 1.   Pressure de-rating factors for PVC (Pisces Pipe Systems)

Temperature (°C)	Pressure de-rating factor
20	1.00
30	0.80
40	0.58
50	0.39
60	0.22

During testing, the temperature inside one of the pressure vessels would be monitored using a temperature sensor. This temperature should not exceed 40°C. At higher temperatures, the rated gauge pressure would fall under 3.5 bars and the vessels would risk being damaged. If the temperature in the pressure vessels rose too high, rock wool or another insulating material could be placed inside the pressure vessels, between the hot heat exchangers and the vessels inner walls, in order to prevent overheating.

Holes with a diameter of 50 mm were drilled at the center of each of the end plugs, and ABS flanges with pipe fittings having a 50 mm inner diameter were mounted on the plugs to allow connecting the pressure vessels to the feedback loop. Sealing was achieved by applying room temperature vulcanizing silicone sealant between the plugs and flanges. The sealant used was manufactured by Granville and capable of withstanding temperatures up to 250°C. The flanges were purchased from eBay Germany and the manufacturer was unknown. According to British retailer Pipestock, ABS pipes and fittings can be used at temperatures between -40°C and 80°C (Pipestock Limited 2012). A Schrader valve and a pressure gauge were also mounted on one of the pressure vessels, to allow pressurizing the engine. Sealing was achieved by using bonded seals, PTFE tape and high temperature Super Glue.

The feedback loop was built using polypropen pipes with an outer diameter of 50 mm and matching elbows and T-branch fittings by Finnish manufacturer KWH Pipe. According to the manufacturer, the pipes can withstand a continuous exposure to temperatures up to 85°C, and up to 100°C over a short time period (KWH Pipe 2010, p. 4). No information was provided regarding the maximum pressure rating, but the wall thickness was known to be 1.8 mm. Sealing was achieved by applying lubricating gel and duct tape to the junction between the pipes and the pressure vessels flanges.

The feedback loop was dimensioned so that the wave generated in the engine would have a frequency of about 120 Hz, which was the resonance frequency of the loud-

speaker. The average temperature in the feedback loop was expected to be about 30°C, slightly higher than room temperature. At this temperature and at a frequency of 120 Hertz, the wavelength was found to be about 2.91 meters (Equations 2.16, 2.17 and 2.21). Note that the speed of sound and the wavelength are independent of pressure, as the p_m terms in Equations 2.16 and 2.17 cancel each other. The different feedback loop sections were dimensioned so that the total length of the engine's loop, including the pressure vessels, would be about 3 meters. Acoustic losses and cross-section enlargements in the pressure vessels may cause the wavelength to differ slightly from the actual length of the engine's loop. Thus, in order to reach a frequency of 120 Hertz, the engine will have to be fine-tuned during testing by adjusting the feedback loop pipes' length.

3.1.2   Heat exchangers

The prototype was originally designed to run on hot water provided by a solar evacuated tubes collector, while cooling would be provided by tap water. Eight identical aluminium crossflow heat exchangers were purchased to be used in the engine's four stages. The heat exchangers were similar to car radiators and measured 158 by 120 by 30 mm without the hose connectors, which were about 12 mm long and had a diameter of 9.3 mm. The corrugations had a density of 18 fins per inch, about 7.3 fins per cm. Each heat exchanger weighed about 212 grams. The main dimensions are given in Figure 14.
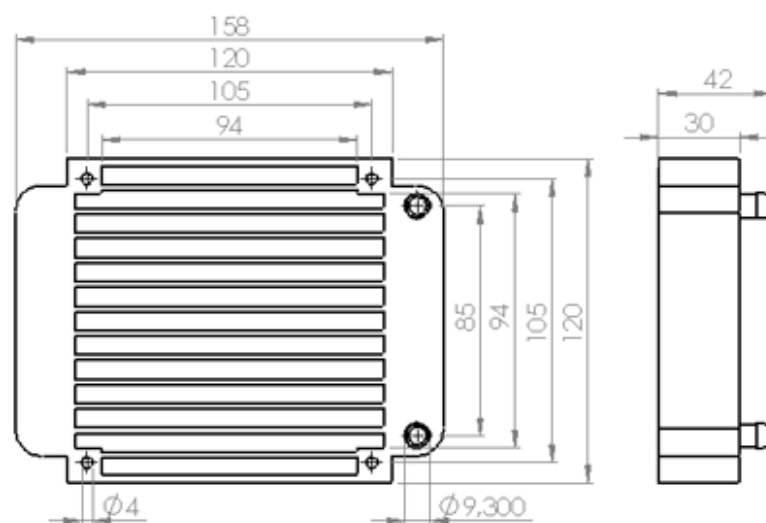

Figure 14.   Main dimensions (in mm) of the heat exchangers. The corrugations are not shown in this drawing.

Cooling was provided by tap water. Rubber hoses with an inner diameter of 8 mm and a wall thickness of 2 mm were used to transport cooling water to and from the engine's low temperature heat exchangers. In addition, 3/8 inch nickel plated brass braided hose connectors were mounted on each pressure vessel to connect the cooling circuit hoses inside and outside of the pressure vessels while maintaining a good pressure seal. Hose connectors inside and outside pressure vessels were fitted together using brass socket fittings. PTFE tape was wrapped around the connectors threads and high temperature silicone sealant was applied at the base of the socket fittings in order to ensure a good seal.

The heating circuit should have been identical to the cooling circuit, except that heat-resistant nitrile rubber pipes would have been used instead of the standard rubber pipes. However, at the time the engine was tested it could not be connected to the solar evacuated tube collector, as the latter had not yet been filled with water. Instead, four soldering iron heating elements were inserted into each of the four hot heat exchangers. The heating elements were made of a Nichrome wire resistance wound inside a 64 mm long and 4 mm large ceramic cylinder. The four heating elements inserted into each hot heat exchanger were connected in series. The total resistance of each of the heating elements sets ranged from 82.6 to 100.0 Ohms. The four sets were then connected in parallel and powered with 230 Volts AC current.

3.1.3   Regenerators

The regenerators were made from stacked stainless steel mesh screens. The mesh was selected so that the hydraulic diameter of the regenerators' channels would be a relatively large fraction of the thermal penetration depth. At a temperature of 300 Kelvins, dry air has a thermal conductivity of $2.624 \cdot 10^{-2}$ $W \cdot m^{-1} \cdot K^{-1}$, a dynamic viscosity of $1.846 \cdot 10^{-5}$ $kg \cdot m^{-1} \cdot s^{-1}$ and a specific heat capacity at a constant pressure of $1.0049 \cdot 10^{3}$ $J \cdot kg^{-1} \cdot K^{-1}$ (Mayhew and Rogers 1995, p. 16). For acoustic oscillations in dry air having a frequency of 120 Hertz, the thermal penetration depth was found to range from about 244 µm at atmospheric pressure to about 123 µm at 3 bars gauge pressure (Equation 2.38). The mesh selected for the regenerators had a wire diameter of 60 µm while the openings were 120 by 120 µm. The mesh number was found to be about 5.6 $mesh \cdot mm^{-1}$ and the porosity about 74% (Equation 2.42). The hydraulic diameter was calculated to be about 43 µm (Equation 2.41), a relatively large fraction of the thermal penetration depth. Figure 15 shows a picture of the mesh taken with a microscope.
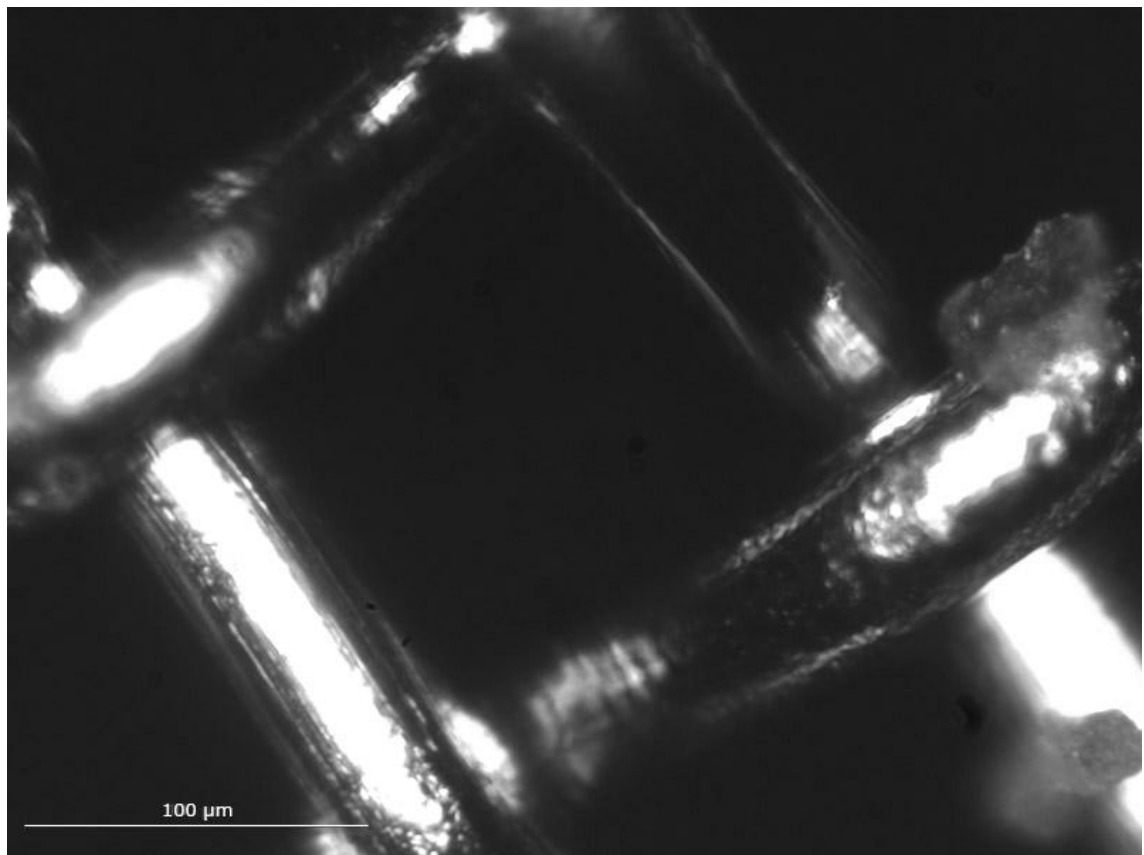
Figure 15.   Microscopic view of the mesh used to make the regenerators

The mesh screens used to build the regenerator had a diameter of 98 mm and were placed inside aluminium pipe section with an inner diameter of 98 mm and an outer diameter of 102 mm. Assuming that the pressure oscillation amplitude in the feedback loop would range from 2 to 5 % of the absolute mean pressure, the particle volumetric flow rate, which should be constant throughout any section of the engine, was found to range from about $0.84 \cdot 10^{-4}$ m^3 at a 2 % drive ratio and at atmospheric mean pressure to about $2.11 \cdot 10^{-4}$ m^3 at a 5 % drive ratio and at a 3 bars gauge pressure (Equation 2.31). Knowing this, the particle displacement amplitude in the regenerator section was found to range from about 1.5 mm at a 2 % drive ratio and at atmospheric pressure to 3.7 mm at a 5 % drive ratio and at a 3 bars gauge pressure (Equation 2.37). The particle displacement amplitude is typically a large fraction of the regenerator's length. In this case, the optimal regenerator length was thought to be about 15 mm and as many as 125 mesh screens were used for each regenerator.

3.1.4   Alternator

The alternator was built using a paper cone loudspeaker with a diameter of 78 mm and a resonance frequency of 120 Hz. The loudspeaker was placed inside a PVC-U drainage pipe socket similar to the ones housing the heat exchangers and regenerators, but with a nominal diameter of 160 mm. Matching end plugs were used to close the socket, and an ABS flange was mounted on one of the plugs to allow connecting the alternator to the feedback loop.

3.2   Sensors and data acquisition system

The performance of a thermoacoustic engine is typically assessed based on the acoustic power output as a function of the temperature gradient across the regenerator. This requires measuring the temperatures on both sides of one of the regenerators in addition to the pressure oscillation amplitude, from which the acoustic power can be calculated. The temperature of air near the pressure sensor and inside one of the pressure vessels, the frequency of oscillation, the volumetric flow rate of water in the cooling circuit and the temperatures of the cooling water flowing in and out of one of the cold heat exchangers were also recorded. The sensors were read using an Arduino: an open-source electronic prototyping platform that comprises a single-board microcontroller and an integrated development environment for programming it.

3.2.1   Measurement of the temperature gradient across the regenerator

A pair of type-K thermocouples and thermocouple amplifier MAX31855 breakout boards were purchased from the online retailer Adafruit Industries to measure the temperatures on both sides of one of the regenerators. Thermocouples consist of two different metal alloys, in this case Nickel-Chromium and Nickel-Aluminium, wound around each other. A slight voltage can be measured between the ends of the two wires. This voltage is temperature-dependent, increasing with increasing temperatures and thus provides a measurement of the temperature. A major advantage of thermocouples over other temperature sensors is that they can be used over a very large temperature range. The two thermocouples used to measure temperatures on the sides of the regenerator had a working temperature range of -100 °C to 500 °C, with a precision of ±2 °C. Thanks to their simple design, thermocouples are also relatively cheap. However, because the voltage change to be measured is very small, a thermocouple amplifier is

required to read them. MAX31855 mounted on breakout boards were used to read the two thermocouples used in this thesis project. A thermocouple connected to a MAX31855 breakout board is shown in Figure 16.
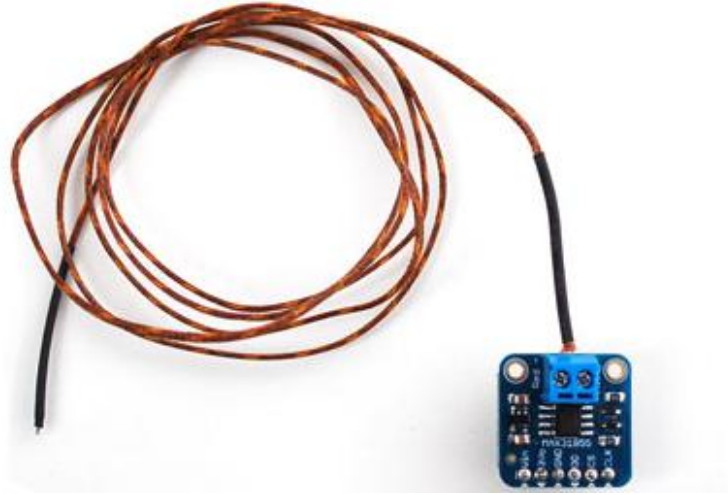

Figure 16.   Thermocouple and amplifier MAX31855 mounted on a breakout board (Image courtesy of Adafruit Industries)

The breakout MAX31855 boards have six pins: Vin, 3Vo, GND, DO, CS and CLK. The Vin pin was connected to a 5 Volts DC breadboard power supply and the GND pin was connected to the ground. The 3Vo pin was not used in this project. The three remaining pins were each connected to digital input pins on the Arduino, as shown in Figure 17.
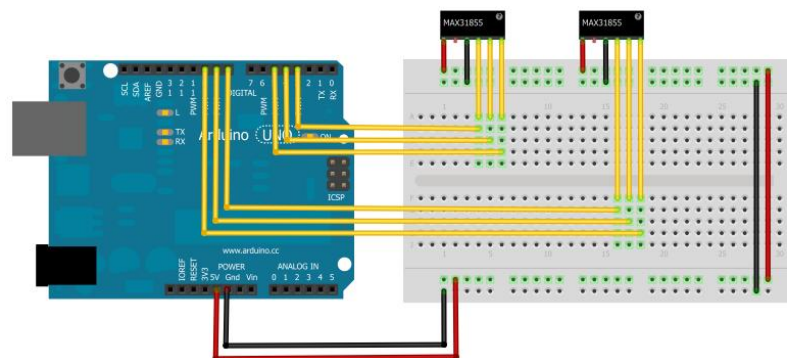

Figure 17.   Wiring diagram of the MAX31855 breakout boards on the Arduino

Note that, in Figure 17, the MAX31855 are connected to the Arduino built-in power supply instead of an external breadboard power supply.

Using the MAX31855 requires downloading and installing the Arduino library code of the same name. With the library installed, the temperature (in °C) of a thermocouple can simply be read using the command `thermocouple.readCelsius()` in the Arduino IDE.

3.2.2   Other temperature measurements

The temperature of cooling water flowing in and out of one of the cold heat exchangers, the air temperature inside one of the pressure vessels, and the air temperature near the pressure sensor were measured using thermistors. Thermistors are resistors whose resistance value changes drastically with temperature. They have a much smaller working temperature range than thermocouples, but can be read directly with a microcontroller without the need for an amplifier. They are also remarkably cheap. The four thermistors used in this thesis project were purchased for 1.50 to 2.00 Euros each. They had a maximum working temperature of 105 °C. The resistance value at 25 °C was 10 kΩ ±1 % and the $\beta_{25/50}$ parameter was 3950 ±1 %. The temperature vs. resistance table of the thermistors is given in Appendix 1.

Each of the thermistors was connected in series to a 10 KΩ resistance mounted on a breadboard to form a voltage divider. A 3.3 Volts DC electrical current was supplied to the thermistors using an external breadboard power supply while the voltage between each thermistor and 10 KΩ resistance was read using the analogue-digital-converter on the Arduino. The wiring diagram of the four thermistors is shown in Figure 18.
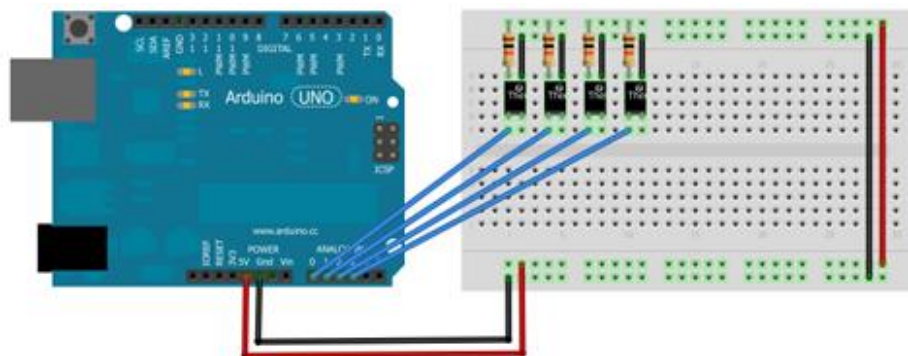

Figure 18.   Wiring diagram of thermistors on the Arduino

Note that, in Figure 18, the thermistors are connected to the Arduino built-in power supply instead of an external breadboard power supply.

As the resistance values of the thermistors change with temperature, so do the voltage values. The resistance value R_1 of each thermistor is given by

$$R_1 = \frac{10 \text{K}\Omega}{\frac{1023}{ADC_{value}} - 1}$$
(3.1)

where ADC_{value} is the value read from the analogue input of the Arduino. Knowing the value of the $\beta_{25/50}$ parameter, the resistance value can be converted to temperature using the β-parameter equation:

$$\frac{1}{T_1} = \frac{1}{T_0} + \frac{1}{\beta_{25/50}} \ln\left(\frac{R_1}{R_0}\right)$$
(3.2)

where T_1 is the temperature measured by the thermistor, T_0 is the reference temperature (25 °C) and R_0 the reference resistance value (10 KΩ). To get more precise readings, five temperature readings were sampled and averaged for each measurement.

3.2.3 Measurement of acoustic pressure amplitude

The frequency of oscillation of the acoustic wave produced in the engine was expected to be about 120 Hertz. To get an accurate reading of the pressure oscillation amplitude inside a wave at this frequency, a pressure sensor capable of taking at least 1000 samples per second was required. A Freescale MPXH6400AC6U temperature compensated analogue pressure sensor was used to measure the pressure oscillation amplitude inside the acoustic wave. This sensor is capable of measuring absolute pressures ranging from 20 to 400 kPa with a maximum error of 1.5 % of the measured value over the temperature range 0 to 85 °C. It has a maximum operating temperature of 125 °C and a response time of 1.0 ms. The MPXH6400AC6U was mounted on a breakout board and placed inside the feedback loop, at approximately 25 cm from one of the hot heat exchangers. The wiring diagram provided by the manufacturer is shown in Figure 19.
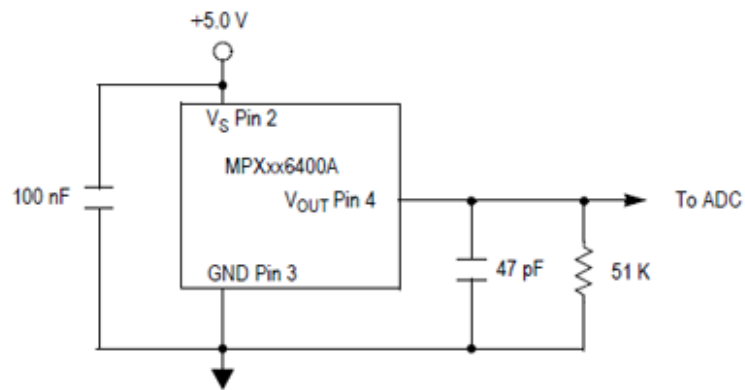
Figure 19.   Wiring diagram of the MPXH6400AC6U pressure sensor (Image courtesy of Freescale Inc.)

The actual wiring on the Arduino is shown in Figure 20.
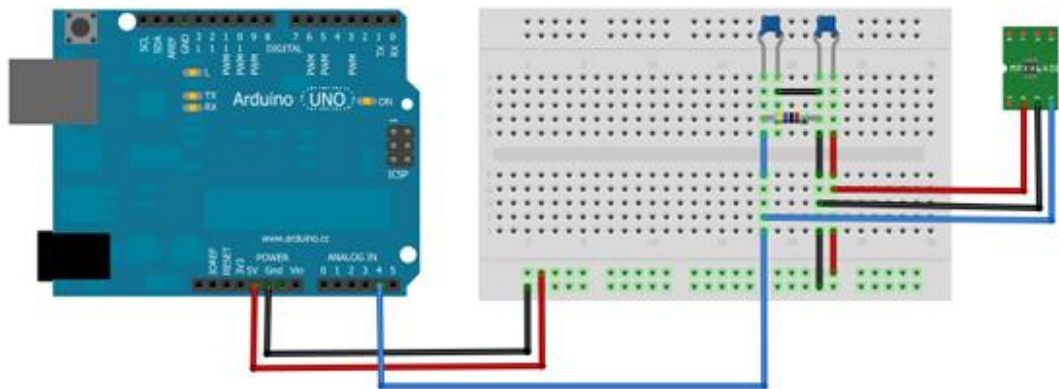
Figure 20.   Wiring of the MPXH6400AC6U on the Arduino

Note that, in Figure 20, the MPXH6400AC6U is connected to the Arduino built-in power supply instead of an external breadboard power supply.

Like thermistors, the MPXH6400AC6U is an analogue sensor and must be read using the ADC on the Arduino. The relation between output voltage and pressure is shown in Figure 21.
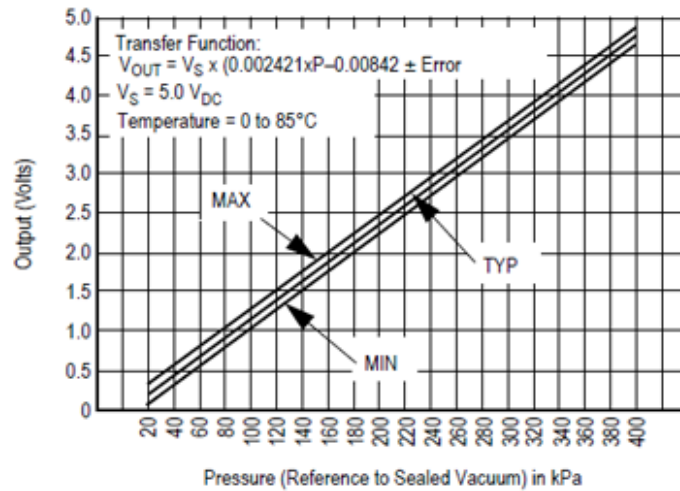
Figure 21.   Output voltage as a function of pressure (Image courtesy of Freescale Inc.)

The sensor was wired according to the manufacturer's instruction, with Pin 2 connected to a 5 Volts DC breadboard power supply, Pin 3 connected to ground and Pin 4 connected to one of the analogue inputs on the Arduino.

The output voltage V_{OUT} of the sensor was calculated by multiplying the value given by the analogue input by the power supplied to the sensor (5 Volts DC) and dividing it by 1023:

$$V_{OUT} = \frac{ADC_{value} \cdot 5 \text{ Volts}}{1023} \tag{3.3}$$

Knowing the sensor's output voltage, the pressure was calculated using the transfer function provided by the manufacturer in Figure 21:

$$p = \frac{V_{OUT}}{5 \text{ Volts} \cdot 0.002421} + \frac{0.00842}{0.002421} \tag{3.4}$$

3.2.4   Measurement of frequency

A piezoelectric disc was inserted in the engine's feedback loop, at approximately 25 cm from one of the hot heat exchangers. Piezoelectric elements are made from materials that generate a voltage in response to mechanical stress. Piezoelectric discs are inexpensive and compact components often encountered in electronic devices where they are used as loudspeakers or as noise sensors. Here the piezoelectric disc works as a

miniature alternator that produces an alternating current as the disc is deformed by acoustic waves in the engine. The frequency of the wave in the engine can then be measured simply by reading the frequency of the current produced by the piezoelectric disc with a multi-meter.

3.2.5 Measurement of cooling water volumetric flow rate

The volumetric flow rate of cooling water was measured using a water flow sensor purchased from Cooking Hacks. The sensor had a working range of 1 to 30 liters per minute with a precision of ±3 % over the range 1 to 10 liters per minute. The maximum working temperature was 80 °C. The sensor consisted of a valve body with 20 mm threaded connectors and a hall-effect sensor mounted on a plastic fan. The fan inside the sensor can be seen in Figure 22.

Figure 22.   Inside view of the flow sensor (Image courtesy of Seeed Studio)

As water flows through the sensor, it spins the fan. With every fan rotation, the hall-effect sensor sends a pulse signal that can be read with one of the digital input pins on the Arduino. The sensor had three wires: black, red and yellow. The black wire was connected to the ground. The red wire was the voltage supply and was connected to a 5 Volts DC breadboard power supply. The yellow wire was the signal and was connected to one of the digital input pins on the Arduino. The wiring diagram of the sensor is shown in Figure 23.

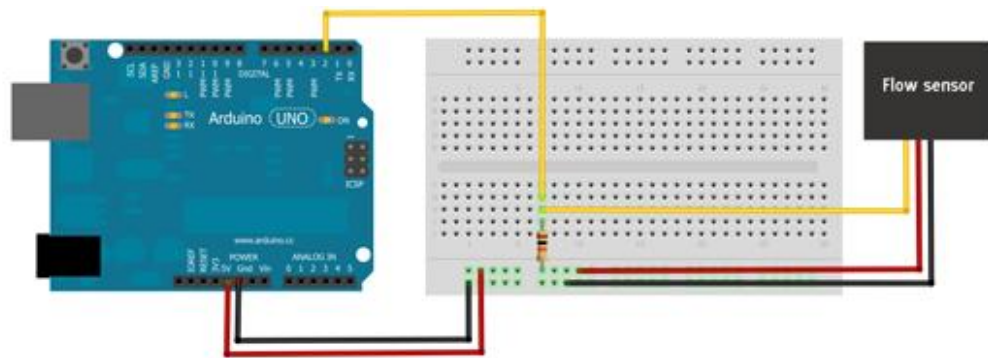Figure 23.   Wiring diagram of the flow sensor on the Arduino

Note that, in Figure 23, the flow sensor is connected to the Arduino built-in power sup-ply instead of an external breadboard power supply.

The signal pulses were detected using the `attachInterrupt()` function. The flow rate in liters per second was then calculated by measuring the number of pulses in one second and dividing it by 7.5.

4 Experimental procedure

The thermoacoustic engine prototype built for this thesis project will later be tested at four different internal mean pressures (ranging from atmospheric to 3 bars gauge pressure) and with one, two, three and four regenerator units in order to measure how these parameters affect the performance of a low cost engine. This chapter details how performance and efficiency will be determined based on data collected during the tests. The results will be published in a separate document.

4.1 Performance

The temperature difference across the regenerator(s) will be calculated from the temperatures measured on both sides of one of the regenerators. The pressure oscillation amplitude will be found by subtracting the mean pressure value from the maximum pressure amplitude recorded at a certain time. The temperature near the pressure sensor will also be recorded and will serve to determine the mean density (Equation 2.17) and thus the speed of sound (Equation 2.16) and the characteristic acoustic impedance (Equation 2.31) of the medium near the pressure sensor. Knowing the characteristic acoustic impedance and the pressure oscillation amplitude, the particles velocity amplitude will be calculated using Equation 2.31. Once both the pressure and the particles velocity oscillation amplitudes are known, the acoustic power in the engine can be determined using Equation 2.33. For each of the sixteen experiments, the acoustic power will be plotted as a function of the temperature difference across the regenerator. In total, sixteen power versus temperature difference curves will be obtained, which will provide a good insight of how the internal mean pressure and number of regenerator units affect the engine's performance. A schema of the four different configurations is shown in Figure 24.
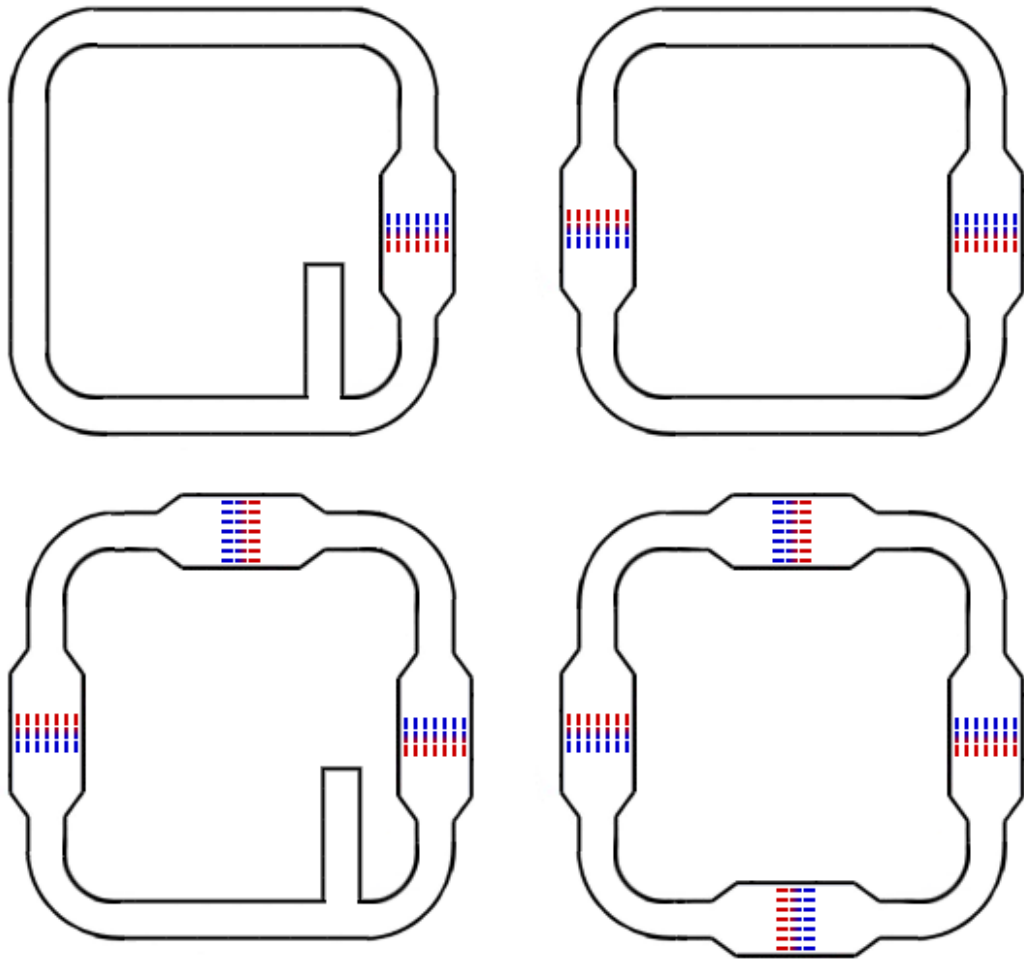
Figure 24.   Four different configurations that will be tested

When an odd number of regenerators is used, an extra volume has to be added to the feedback loop after the last hot heat exchanger, in order to lower the acoustic impedance and allow oscillations to start. This is done simply by adding an extra pipe section at a distance of about one tenth of the wavelength from the last hot heat exchanger. The extra section has a length of about one tenth of the wavelength.

4.2   Efficiency

The theoretical upper limit for a heat engine's efficiency is defined as the Carnot efficiency:

$$\eta_{Carnot} = 1 - \frac{T_C}{T_H} \qquad (4.1)$$

where T_C is the temperature (in Kelvins) on the cool side of the regenerator and T_H that on the hot side of the regenerator.

The actual engine's overall efficiency will be calculated by dividing the acoustic power $\bar{P}_{ac}$ produced once the hot heat exchangers have reached their maximum temperature by the amount of electrical power $\bar{P}_{el}$ consumed by the heating elements:

$$\eta = \frac{\bar{P}_{ac}}{\bar{P}_{el}} \tag{4.2}$$

The electrical power consumed by the heating elements can easily be calculated by dividing the squared of the RMS value of the voltage V supplied by the total electric resistance R of the elements:

$$\bar{P}_{el} = \frac{\left(\frac{1}{\sqrt{2}}V\right)^2}{R} = \frac{V^2}{2R} \tag{4.3}$$

It is important that this measurement be done once the engine has reached steady state, that is, once the hot heat exchangers have reached their maximum temperature and this temperature remains stable over time. In transient state, part of the electrical power supplied to the heating elements is used to raise the temperature of the heat exchangers, thus giving a false reading of the actual efficiency.

The efficiency of a heat engine is also typically expressed as a percentage of the Carnot efficiency:

$$e = \frac{\eta}{\eta_{Carnot}} \cdot 100 \tag{4.4}$$

5 Conclusions and future work

Thermoacoustics is a relatively new field of physics that combines acoustics, thermo-dynamics and fluid dynamics to describe the interplay between heat and sound. Since the late sixties, research in this area has yielded devices capable of converting part of the heat flowing through a temperature gradient into large amplitude sound waves and vice-versa with efficiencies now close to those of established technologies. In recent years, thermoacoustic engines, heat pumps and refrigerators have been gaining a lot of attention due to their inherent mechanical simplicity and to their use of environmen-tally friendly working gases. One of the most promising areas of application for these devices seems to be the use of low temperature industrial waste heat. This thesis fo-cused on the design and assembly of a low cost traveling wave thermoacoustic engine prototype intended to be used for low temperature waste heat recovery. This prototype will allow measuring how different parameters affect the performance of a low cost en-gine, in search for an optimal configuration. This thesis was divided into two main parts: chapter 2 covering the necessary theoretical background required to dimension the engine and chapter 3 documenting the dimensioning, components selection and as-sembly of the prototype. Chapter 4 then briefly described how the prototype will be tested in order to measure how two parameters, internal mean pressure and number of regenerator units, influence the engine's performance.

Time management has been a major issue in this project and the main reason behind the fact that the prototype could not be tested soon enough for the results to be pub-lished in this thesis. Only a raw draft of the prototype had been made when the project started and many elements in the design of the engine had to be re-thought, either be-cause the required parts were no longer available or because it later became apparent that they were not adequate for this prototype. The schedule submitted at the begin-ning of the project allocated two weeks for finding the required components. In reality, re-thinking the design of the engine, looking for appropriate parts and having them shipped to Finland took close to three months. When the time of testing the engine finally came, problems were encountered with the heating elements supposed to pro-vide heat to the engine. The heating elements had been designed simply using re-sistance wire and winding it around the hot heat exchangers. But the aluminium heat exchangers would short-circuit the resistances, preventing them from heating up. A second design using resistance wire wound around M6 stainless steel threaded rods covered with ceramic beads to prevent short circuits was assembled. Once again,

shorts circuits would occur as the resistance wire would "slip" on the ceramic beads when manipulating the engine and parts of the wire would happened to touch each other. A third and final configuration was built using soldering iron heating elements. Four heating elements were inserted into each of the hot heat exchangers. This configuration was tested with a laboratory DC power supply and seemed to be working properly, only the power supplied was insufficient and the temperature of the hot heat exchangers would not exceed 45°C. This configuration will later be tested using 230 Volts AC current from the grid, which will hopefully be sufficient to bring the temperature of the hot heat exchangers up to at least 100°C. On the positive side, the total budget for the prototype including the Arduino and sensors was kept below 1 500 Euros, as promised at the beginning of the project.

The next step is now to perform the tests detailed in chapter 4 and to draw conclusions about how internal mean pressure and number of regenerators affect the engine's performance. Based on previous studies, it is expected that the dependency of acoustic power on internal mean pressure will be non linear, so that the rate at which acoustic power increases with increasing internal mean pressure will tend to decrease with increasing internal mean pressure and to eventually reach an optimum. Finding this optimum is essential as a high internal mean pressure leads to a greater capital cost as stronger materials have to be used. However, this prototype was designed to withstand a maximum gauge pressure of 3 bars and the optimum may turn out to be higher than that, in which case it may be necessary to build a new prototype with more robust materials capable of withstanding a higher internal mean pressure. How exactly the performance will be affected by the number of regenerators is yet unknown, although there again it can be expected that an optimal configuration exists, after which acoustic losses inside the regenerators will offset their beneficial effect on acoustic gain. A maximum of four regenerators will be used during the tests, and as for internal mean pressure, the optimal configuration may turn out to require a larger number of regenerators, in which case the prototype will have to be upgraded. Finally, it may be interesting to test the engine with different working gases, bearing in mind that the regenerator's mesh may have to be changed to maintain the desired ratio between the mesh's hydraulic diameter and the gas's thermal and viscous penetration depths.

References

Beyer, RT 1999, *Sounds of Our Times: two hundred years of acoustics*, Springer-Verlag, New-York.

Crowell, B 2002, *Vibrations and Waves*, edition 2.1, Fullerton.

De Blok, K 2010, "Novel 4-stage traveling wave thermoacoustic power generator", *Proceedings of ASME 2010 3rd Joint US-European Fluids Engineering Summer Meeting and 8th International Conference on Nanochannels, Microchannels, and Minichannels*, ASME, Montreal.

In't panhuis, PHMW 2009, "Mathematical Aspects of Thermoacoustics", PhD thesis, Eindhoven University of Technology, Eindhoven.

KWH Pipe, 2010, *WehoPropen käsikirja*, viewed 19 June 2012, <http://www.kwhpipe.fi/Link.aspx?id=519878>

Mayhew, YR & Rogers GFC 1995, *Thermodynamic and Transport Properties of Fluids*, 5th edition, Blackwell, Oxford.

Morin, D 2011, *Oscillations*, viewed 20 May 2012, <http://www.people.fas.harvard.edu/~djmorin/waves/oscillations.pdf>

Morris, J, *Under pressure*, New Zealand Water and Environment Training Academy, viewed June 19 2012, <http://www.nzweta.org.nz/page49921.html>

Pipestock Limited, 2012, *ABS Specifications*, viewed 19 June 2012, <http://www.pipestock.com/abs-specifications/>

Pisces Pipe Systems, *Technical information and FAQ*, viewed 19 June 2012, <http://www.pisces-aqua.co.uk/technical/FAQ/index.htm#Temperature rating of pvc and abs pipework>

Plomyplas Group, *PVC-U pressure pipes systems*, viewed 19 June 2012, <http://www.plomyplas.com/images/archivos/im0156_0_catalogo_duronil_en_ingles.pdf>

Rijke, PL 1859, "Notice of a New Method of causing a Vibration of the Air contained in a Tube open at both ends", *The London, Edinburgh and Dublin Philosophical Magazine and Journal of Science*, vol. 17, Fourth series, pp. 419-422

Sirci Gresintex, *PVC-KG Rohre und Formstücke für Abwasserleitungen*, viewed 19 June 2012, <http://www.seiter-europe.de/pdf/formstuecke.pdf>

Swift, GW 2002, *Thermoacoustics: A unifying perspective for some engines and refrigerators*, Acoustical Society of America, Melville NY.

Wolfson, R 2012, *Essential University Physics*, vol. 1, 2nd edition, Addison Wesley, San Francisco.

Temperature vs. resistance table of the thermistors

热 敏 电 阻 电 阻 — 温 度 分 度 表

R（25℃）：10KΩ   B(25℃/50℃):3950

T（℃）	R（kΩ）	T（℃）	R（KΩ）	T（℃）	R（kΩ）	T（℃）	R（kΩ）
−25	133.500	15	15.7511	55	2.96331	95	.781670
−24	125.672	16	15.0306	56	2.85569	96	.758701
−23	118.350	17	14.3472	57	2.75256	97	.736519
−22	111.498	18	13.6987	58	2.65369	98	.715094
−21	105.084	19	13.0833	59	2.55890	99	.694397
−20	99.0773	20	12.4990	60	2.46799	100	.674400
−19	93.4469	21	11.9441	61	2.38080	101	.655075
−18	88.1750	22	11.4169	62	2.29714	102	.636398
−17	83.2296	23	10.9161	63	2.21686	103	.618345
−16	78.5909	24	10.4400	64	2.13980	104	.600890
−15	74.2384	25	10.0000	65	2.06583	105	.584013
−14	70.1527	26	9.55693	66	1.99480	106	.567690
−13	66.3162	27	9.14743	67	1.92658	107	.551902
−12	62.7122	28	8.75777	68	1.86105	108	.536629
−11	59.3254	29	8.38690	69	1.79809	109	.521852
−10	56.1416	30	8.03380	70	1.73758	110	.507552
−9	53.1475	31	7.69753	71	1.67942	111	.493712
−8	50.3307	32	7.37721	72	1.62351	112	.480316
−7	47.6799	33	7.07200	73	1.56975	113	.467346
−6	45.1842	34	6.78110	74	1.51804	114	.454788
−5	42.8339	35	6.50378	75	1.47300	115	.442627
−4	40.6197	36	6.23934	76	1.42045	116	.430848
−3	38.5330	37	5.98711	77	1.37439	117	.419438
−2	36.5656	38	5.74646	78	1.33007	118	.408384
−1	34.7103	39	5.51680	79	1.28740	119	.397674
0	32.9600	40	5.29758	80	1.24632	120	.387294
1	31.3081	41	5.08828	81	1.20675	121	.377233
2	29.7487	42	4.88838	82	1.16864	122	.367481
3	28.2760	43	4.69743	83	1.13193	123	.358026
4	26.8848	44	4.51498	84	1.09655	124	.348859
5	25.5702	45	4.34060	85	1.06246	125	.339968
6	24.3274	46	4.17391	86	1.02960		
7	23.1523	47	4.01452	87	.997924		
8	22.0407	48	3.86207	88	.967376		
9	20.9889	49	3.71624	89	.937916		
10	19.9934	50	3.58800	90	.909498		
11	19.0509	51	3.44314	91	.882083		
12	18.1582	52	3.31529	92	.855630		
13	17.3124	53	3.19287	93	.830101		
14	16.5109	54	3.07563	94	.805459		

Helsinki
Metropolia
University of Applied Sciences